Multi-mechanism models for the description of ratchetting : effect of the scale transition rule and of the coupling between hardening variables

Kacem Sai, Georges Cailletaud

Multi-mechanism models for the description of ratchetting: Effect of the scale transition rule and of the coupling between hardening variables

K. Sai [a,*], G. Cailletaud [b]

[a] *LGPMM, Ecole Nationale d'Ingénieurs de Sfax, BP W 3038, Tunisia*

[b] *Centre des Matériaux UMR/7633, Ecole des Mines de Paris, BP 87 91003 Evry ParisTech, France*

Abstract

This paper is concerned with two multi-mechanism based models for application to ratchetting effect. The 2M1C (2 Mechanisms and 1 Criterion) model and 2M2C (2 Mechanisms and Criteria) model, proposed by the authors in a previous article, are modified to incorporate (i) a corrective term in the computation of the local stresses, (ii) Burlet-Cailletaud's fading memory term in the kinematic hardening evolution rule. Experimental data from the literature are selected to assess the models capability. Numerical results are obtained using the proposed models for a series of uni-axial and multi-axial ratchetting tests performed at different stress ranges of an austenitic stainless steel.

Key words: Multi-mechanism modeling, Ratchetting behavior, Nonproportional loading, Additional hardening

* Corresponding Author. E-mail adress: kacemsai@yahoo.fr

Nomenclature

Variables:

$\dot{\underset{\sim}{\varepsilon}}$: total strain rate

$\dot{\underset{\sim}{\varepsilon}}^{e}$: elastic strain rate

$\dot{\underset{\sim}{\varepsilon}}^{p}$: overall plastic strain rate

$\dot{\underset{\sim}{\varepsilon}}^{I}$: inelastic strain rate for mechanism I

$\underset{\sim}{\sigma}$: overall stress tensor

$\underset{\sim}{\sigma}^{I}$: local stress tensor for mechanism I

$\underset{\sim}{\beta}^{I}$: accommodation variable for mechanism I

$\underset{\sim}{\alpha}^{I}$: kinematic internal variable for mechanism I

r^{I}: isotropic internal variable for mechanism I (2M2C model only)

r: isotropic internal variable (2M1C model only)

$\dot{\lambda}^{I}$: inelastic multiplier for mechanism I (2M2C model only)

$\dot{\lambda}$: inelastic multiplier (2M1C model only)

$\underset{\sim}{\mathbf{n}}^{I}$: normal to the yield surface for mechanism I

$\underset{\sim}{\mathbf{X}}^{I}$: back stress for mechanism I

R^{I}: size change of the elastic domain for mechanism I (2M2C model only)

R: size change of the elastic domain (2M1C model only)

Material parameters:

$\underset{\sim}{\mathbf{B}}^I$: stress concentration tensor

μ: elastic shear modulus

μ': localization parameter

$(1-z)$, z: weighting factors of the two mechanisms respectively

C_{11}, C_{12}, C_{22}; $[C]$: kinematic hardening moduli; interaction matrix

D_I: kinematic hardening parameter for mechanism I

δ_I: additive kinematic hardening parameter for mechanism I

d_I: parameter of the accommodation variable for mechanism I

R_0^I: initial size of the elastic domain for mechanism I (2M2C model only)

R_0: initial size of the elastic domain (2M1C model only)

Q_I, b_I: isotropic parameters for mechanism I (2M2C model only)

Q, b: isotropic parameters (2M1C model only)

Introduction

In the last two decades, a series of studies have been proposed to model the ratchetting phenomenon. Ratchetting (that is accumulation of inelastic strain) occurs during onedimensional cyclic loading in the presence of a mean stress. Strain ratchetting under biaxial loading involves a (generally symmetric)

loading on a given component, meanwhile a constant value is applied on an other component (for instance strain symmetric torsional cycling in the presence of a constant axial load).

Numerous plasticity models have been developed and modifications or new formulations are currently being proposed: ((McDowell, 1995), (Ristinmaa, 1995), (Jiang and Kurath, 1996), (Basuroychowdhury and Voyiadjis, 1998), (Taheri and Lorentz, 1999), (Yoshida, 2000), (Abdel-Karim and Ohno, 2000), (Bari and Hassan, 2000), (Bari and Hassan, 2001), (Bari and Hassan, 2002), (Vincent et al., 2004), (Yaguchi and Takahashi, 2005), (Abdel-Karim, 2005)). These works have been realized on two types of models: (i) the first one is based on the NonLinear Kinematic (NLK) hardening rule (Armstrong and Frederick, 1966). This approach have been extensively worked out by Chaboche (Chaboche and Rousselier,), (Chaboche and Jung, 1997), (Chaboche, 1986), (Chaboche et al., 1991). A non exhaustive list of major modifications of the NLK hardening rule includes the work of (Burlet and Cailletaud, 1987), (Ohno and Wang, 1993b), (Ohno and Wang, 1993a) . . . , (ii) the second kind of model is based on multi-surface theory (Mroz, 1967) (Krieg, 1975) (Dafalias and Popov, 1976).

In addition, several experimental studies describing the investigation of ratchetting behavior are available (Yoshida, 1989), (Ruggles and Krempl, 1989), (Delobelle et al., 1995), (Ohno et al., 1998), (Mizunno et al., 2000), (Bocher et al., 2001), (Kang et al., 2002), (Feaugas and Gaudin, 2004), (Yaguchi and Takahashi,), (Kang et al., 2006). (Jiang and Sehitoglu, 1994a), (Jiang and Sehitoglu, 1994b).

(Hassan et al., 1992b), (Hassan et al., 1992a), (Hassan and Kyriakides, 1994a), (Hassan and Kyriakides, 1994b) have performed experimental tests for 1070, 1018 and 1026 carbon steels. Most of the authors have reported experimental

results on uni-axial and multi-axial ratchetting tests mainly for type 304, 316 and 316L stainless steels. A comparative study has been performed in (Portier et al., 2000): five sets of constitutive equations were selected and their material parameters were identified on a large experimental data base. The tests have been carried out at 25°C and 250°C on a 316 austenitic stainless steel.

The purpose of this article is to offer a third point of view for the description of ratchetting phenomenon. The proposed approach is based upon the investigation of multi-mechanism and multi-criteria models. These models are assumed to depend on n "mechanisms" and m "criteria" and are usually called nMmC. This general framework includes the models proposed by (Zarka and Casier, 1979), (Khabou et al., 1990), (Cailletaud and Sai, 1995), (Zarka and Navidi, 1998) and (Taleb et al., 2006) for 2M1C model type; (Contesti and Cailletaud, 1989) (Cailletaud and Sai, 1995) for 2M2C model type. The newly revisited approach combines the properties of the nMmC models with a more physical concentration rule inspired from the micro-mechanical approach (Cailletaud, 1992), (Cailletaud, 1987), (Cailletaud and Pilvin, 1994), (Sai et al., 2006a) .

Previous works have shown that several mechanical effects can be described by playing on the characteristics of the hardening matrix $[C]$. (Contesti and Cailletaud, 1989) have proposed a 2M2C model type in which one of the two mechanisms is plastic whereas the second is viscoplastic. They have shown that this model is able to describe the inverse rate sensitivity and creep-plasticity interaction. The ratchetting effect is also governed by the numerical value of the determinant of this matrix in the 2M1C model in the case of linear kinematic hardening rule: (Zarka and Casier, 1979) and (Cailletaud and Sai, 1995) have shown that if the matrix $[C]$ is singular, then ratchetting is observed. On the other hand, a regular matrix leads to shakedown. In the present work, this

property will be extended to the 2M2C model.

The paper is organized as follows: in section 1 the main lines of the constitutive equations of the 2M2C and 2M1C models are briefly recalled within their thermodynamical framework. In that section, a particular attention is paid to the correlation between the ratchetting behavior and the properties of the kinematic hardening matrix (this matrix contains the different hardening moduli). Section 2 is devoted to the description of the new features introduced in the model (a scale transition rule inspired from the uniform field models to compute the local stresses, and an improved rule for kinematic hardening). The mechanical and physical origins of this scale transition rule are first explained. A new version of the 2M1C and the 2M2C models is then presented. The capabilities of the modified models are presented in section 3. Two examples are treated with the new models; the ratchetting effect and the additional hardening in out-of-phase loading. In these new models, the modifications are based on:

- the use of the transition rule of the micro-mechanical models (see for instance (Cailletaud and Pilvin, 1994)) in order to control the kinematic hardening matrix characteristics,

- the modification of the fading memory terms according to the model proposed by (Burlet and Cailletaud, 1987) to calibrate multi-axial ratchetting.

To assess the model reliability, a comparison is made in section 4 between the modified 2M1C and 2M2C models and an experimental data base taken from (Portier et al., 2000) for an austenitic stainless steel. A closed form solution of the variation of the maximal axial strain per cycle obtained for various

kinematic rules is finally presented for the 2M2C model (Appendix A).

1 2M2C and 2M1C models: initial version

1.1 Thermodynamical framework

Our goal in this section is to recall the constitutive equations of the multi-mechanism models. It was previously shown (Cailletaud and Sai, 1995) that the form of the constitutive equations of these models is compatible with the general thermodynamical framework developed by (Germain et al., 1983). The construction of a plasticity theory requires in general the definition of (i) a yield function f, (ii) a flow potential Ω and (iii) a hardening potential Ω_h. Within the frame of a generalized standard material (Halphen and Nguyen, 1975), these three functions are defined by means of one potential only. In this particular class of materials, the flow rules defining the (strain like) internal variables are obtained by derivation of the potential with respect to the associated (stress like) hardening variables. The intrinsic dissipation is then the difference between the plastic power and the fraction of power temporarily stored by the hardening mechanisms:

$$\mathcal{D} = \underset{\sim}{\sigma} : \dot{\underset{\sim}{\varepsilon}}^p - \rho\dot{\Psi} = \underset{\sim}{\sigma} : \dot{\underset{\sim}{\varepsilon}}^p - A_I\dot{\alpha}^I \tag{1}$$

As a consequence of the first and the second principle, Clausius-Duhem inequality tells that $\mathcal{D}$ must be positive. This is the case if and only if $\Omega \equiv \Omega_h$ and Ω is convex. The free energy $\rho\Psi$, used as a potential, defines stress and hardening variables knowing elastic strain and internal variables (where ρ is

the density of the material):

$$\underset{\sim}{\sigma} = \rho \frac{\partial \Psi}{\partial \underset{\sim}{\varepsilon}^e} \quad \text{and} \quad A_I = \rho \frac{\partial \Psi}{\partial \alpha^I} \tag{2}$$

Assuming uncoupling between elastic and plastic part, Ψ can be considered as the sum of two contributions: an elastic one (Ψ_e) and a plastic one (Ψ_p):

$$\Psi = \Psi^e + \Psi^p \tag{3}$$

From a thermodynamical point of view, the starting point of the multi-mechanism models is a collection of potentials $\Omega^I, I = 1..N$ (where N is the number of the considered mechanisms). For each mechanism I, a local stress $\underset{\sim}{\sigma}^I$ is obtained through a concentration tensor $\underset{\approx}{\mathbf{B}}^I = \frac{\partial \underset{\sim}{\sigma}^I}{\partial \underset{\sim}{\sigma}}$. Note that for the initial version of the models, $\underset{\approx}{\mathbf{B}}^I = \underset{\approx}{\mathbf{I}}$ has been chosen. Two cases have been distinguished, in the multi-mechanism models:

- Each $\underset{\sim}{\sigma}^I$ is involved in a different yield functions f^I, defining a series of different criteria:

$$\dot{\underset{\sim}{\varepsilon}}^p = \sum_I \frac{\partial \Omega^I}{\partial \underset{\sim}{\sigma}} = \sum_I \frac{\partial \Omega^I}{\partial f^I} \frac{\partial f^I}{\partial \underset{\sim}{\sigma}} = \sum_I \frac{\partial \Omega^I}{\partial f^I} \frac{\partial f^I}{\partial \underset{\sim}{\sigma}^I} : \frac{\partial \underset{\sim}{\sigma}^I}{\partial \underset{\sim}{\sigma}} = \sum_I \frac{\partial \Omega^I}{\partial f^I} \underset{\sim}{\mathbf{n}}^I : \underset{\approx}{\mathbf{B}}^I \tag{4}$$

  This includes the 2M2C model and the crystal plasticity models. For these models, each mechanism has its own inelastic multiplier.

- All $\underset{\sim}{\sigma}^I$ are combined into an unique global criterion f:

$$\dot{\underset{\sim}{\varepsilon}}^p = \frac{\partial \Omega}{\partial \underset{\sim}{\sigma}} = \frac{\partial \Omega}{\partial f} \frac{\partial f}{\partial \underset{\sim}{\sigma}} = \frac{\partial \Omega}{\partial f} \sum_I \frac{\partial f}{\partial \underset{\sim}{\sigma}^I} : \frac{\partial \underset{\sim}{\sigma}^I}{\partial \underset{\sim}{\sigma}} = \frac{\partial \Omega}{\partial f} \sum_I \underset{\sim}{\mathbf{n}}^I : \underset{\approx}{\mathbf{B}}^I \tag{5}$$

  2M1C model belongs to this second class of model, for which only one inelastic multiplier has to be determined.

1.2 2M2C model

The 2M2C model is assumed to depend on two mechanisms and two criteria (yield functions). The inelastic part of the free energy function can be expressed as a function of the internal variables $\underset{\sim}{\alpha}^1$, $\underset{\sim}{\alpha}^2$, r^1 and r^2 as follows:

$$\rho\Psi_p = \frac{1}{3}\sum_I\sum_J C_{IJ}\underset{\sim}{\alpha}^I : \underset{\sim}{\alpha}^J + \frac{1}{2}\sum_I Q_I\left(r^I\right)^2 \tag{6}$$

The hardening variables are then:

$$\underset{\sim}{\mathbf{X}}^I = \rho\frac{\partial\Psi_p}{\partial\underset{\sim}{\alpha}^I} = \frac{2}{3}\sum_J C_{IJ}\underset{\sim}{\alpha}^J \qquad R^I = \rho\frac{\partial\Psi_p}{\partial r^I} = Q_I\, r^I \tag{7}$$

The flow rule is generated by a potential, which is the sum of two terms:

$$\begin{cases} f^I = J(\underset{\sim}{\sigma} - \underset{\sim}{\mathbf{X}}^I) - R^I - R_0^I \qquad \Omega = \Omega^1(f^1) + \Omega^2(f^2) \\ \text{where} \quad J(\underset{\sim}{\sigma} - \underset{\sim}{\mathbf{X}}^I) = \sqrt{\frac{3}{2}(\underset{\sim}{\mathbf{s}} - \underset{\sim}{\mathbf{X}}^I) : (\underset{\sim}{\mathbf{s}} - \underset{\sim}{\mathbf{X}}^I)} \end{cases} \tag{8}$$

So that:

$$\dot{\underset{\sim}{\varepsilon}}^p = \frac{\partial\Omega^1}{\partial f^1}\underset{\sim}{\mathbf{n}}^1 + \frac{\partial\Omega^2}{\partial f^2}\underset{\sim}{\mathbf{n}}^2 \quad \text{with} \quad \underset{\sim}{\mathbf{n}}^I = \frac{\partial f^I}{\partial\underset{\sim}{\sigma}} = \frac{3}{2}\frac{\underset{\sim}{\mathbf{s}} - \underset{\sim}{\mathbf{X}}^I}{J(\underset{\sim}{\sigma} - \underset{\sim}{\mathbf{X}}^I)} \tag{9}$$

In the present form, it can be easily checked that the dissipation (Eq. 1) remains positive. The hardening rules of the 2M2C model are expressed as follows:

$$\dot{\underset{\sim}{\alpha}}^I = \left(\underset{\sim}{\mathbf{n}}^I - \frac{3D_I}{2C_{II}}\underset{\sim}{\mathbf{X}}^{\mathbf{I}}\right)\frac{\partial\Omega^I}{\partial f^I} \qquad \dot{r}^I = \left(1 - \frac{b_I R^I}{Q_I}\right)\frac{\partial\Omega^I}{\partial f^I} \tag{10}$$

The model would be a "generalized standard" model, by taking $D_I = 0$ and $Q_I \to \infty$.

The 2M2C model type allows, for example, the simultaneous treatment of plasticity and viscoplasticity. The plastic formulation leads to time independent

responses whereas the viscoplastic formulation produces relaxation and creep. The model is then able to discriminate between the increase of hardening produced by plasticity or creep. This may be quite important to model complex behaviors like 316 stainless steel at 650°C (Contesti and Cailletaud, 1989) or N-18 alloy in the temperature range 600-700°C (Sai et al., 2004).

The 2M2C model type can also be applied to study phase transformation. In this class of models, a stress tensor and a strain tensor are defined in each phase of the material inside the representative volume element. (Videau et al., 1994) were the first who applied the multi-mechanism models for the phase transformation. In the work of (Gautier and Cailletaud, 2004) and (Sai et al., 2006b) the transformation induced plasticity of a 304 stainless steel is carried out using a multi-mechanism model in which the influence of each phase is balanced by its volume fraction which is calculated by a kinetics transformation rule.

1.3 2M1C model

The 2M1C model is assumed to depend on two mechanisms and one criterion (yield function). The inelastic part of the free energy function can be expressed as a function of the internal variables $\underset{\sim}{\alpha}^1$, $\underset{\sim}{\alpha}^2$ and r as follows:

$$\rho\Psi_p = \frac{1}{3}\sum_I\sum_J C_{IJ}\underset{\sim}{\alpha}^I : \underset{\sim}{\alpha}^J + \frac{1}{2}Qr^2 \tag{11}$$

The relations between the internal variables and their associated forces are:

$$\underset{\sim}{\mathbf{X}}^I = \rho\frac{\partial\Psi_p}{\partial\underset{\sim}{\alpha}^I} = \frac{2}{3}\sum_J C_{IJ}\underset{\sim}{\alpha}^J \qquad R = \rho\frac{\partial\Psi_p}{\partial r} = Qr \tag{12}$$

The evolution laws of these variables are generated by a potential which introduces a quadratic combination of the two mechanisms:

$$f = \left(J(\underset{\sim}{\sigma} - \underset{\sim}{\mathbf{X}}^1)^2 + J(\underset{\sim}{\sigma} - \underset{\sim}{\mathbf{X}}^2)^2\right)^{1/2} - R - R_0 \qquad \Omega \equiv \Omega(f) \tag{13}$$

This form generates a coupling between the two mechanisms that is not considered in the 2M2C model (see Fig. 1). If Ω is a true viscoplastic potential, the viscoplastic strain rate is:

$$\begin{cases} \dot{\underset{\sim}{\varepsilon}}^p = \dfrac{\partial \Omega}{\partial f}\underset{\sim}{\mathbf{n}} = \dfrac{\partial \Omega}{\partial f}\dfrac{J_1\underset{\sim}{\mathbf{n}}^1 + J_2\underset{\sim}{\mathbf{n}}^2}{(J_1^2 + J_2^2)^{1/2}} \\ \text{with} \quad J_I = J(\underset{\sim}{\sigma} - \underset{\sim}{\mathbf{X}}^I) \quad \text{and} \quad \underset{\sim}{\mathbf{n}}^I = \dfrac{3}{2}\dfrac{\underset{\sim}{\mathbf{s}} - \underset{\sim}{\mathbf{X}}^I}{J_I} \end{cases} \tag{14}$$

The partial derivative of Ω with respect to f is simply replaced by a plastic multiplier to write a time independent plastic model. Finally, the hardening rules of the 2M1C model are as follows:

$$\dot{\underset{\sim}{\alpha}}^I = \left(\underset{\sim}{\mathbf{n}}^I - \frac{3D_I}{2C_{II}}\underset{\sim}{\mathbf{X}}^{\mathbf{I}}\right)\frac{\partial \Omega^I}{\partial f^I} \qquad \dot{r} = \left(1 - \frac{bR}{Q}\right)\frac{\partial \Omega}{\partial f} \tag{15}$$

1.4 Summary of the 2M2C and 2M1C models

For both 2M2C and 2M1C model, a kinematic-kinematic coupling is introduced between the hardening variables through the material parameter C_{12}. The detailed equations of the 2M1C model and the 2M2C model (Cailletaud and Sai, 1995) are summarized in Table 1 and Table 2 respectively. The 2M1C model produces one type of flow with the simultaneous activation of the two mechanisms whereas 2M2C model has several regimes, according to stress and strain rate levels.

1.5 Ratchetting effect

Even if the yield criteria are basically different, the 2M1C and 2M2C models keep common characteristics with respect to ratchetting behavior. As previously demonstrated (Cailletaud and Sai, 1995), ratchetting behavior of the 2M1C model is closely related to the hardening matrix (Fig. 2). This property is also applicable for the 2M2C model. It is shown analytically in the Appendix A, for the case of a one dimensional loading that:

- when linear kinematic hardening rules are considered, the ratchetting behavior is controlled by the character of the hardening matrix. If the determinant of this matrix is equal to zero then ratchetting behavior is observed. However, a regular matrix leads to shakedown behavior.

- in the case of non linear kinematic hardening rules, a constant evolution of the tensile peak strain is obtained. The variation of the tensile peak strain between two successive cycles is expressed analytically according to the components of the matrix $[C]$, the fading memory parameters and the applied cyclic stresses (σ_{min}, σ_{max}).

In this initial version, all the mechanisms are submitted to the same macroscopic stress. In order to get closer from a physical situation, it is now proposed to use a scale transition rule, which will reduce local stress on the more deformed mechanisms.

2 New features introduced in the model

2.1 General remarks on the scale transition rules

The aim of this paragraph is to study the effect of the newly introduced transition rule on the ratchetting behavior. Let us refer for a while to crystal plasticity, in order to consider the various types of models developed in this field. Beside the simplest and most widely used models (uniform plastic strain (Taylor, 1938); uniform stress), the most popular concept is the self-consistent framework proposed by (Hill, 1965) and revisited by many authors (see for instance (Molinari, 1999)). In terms of rates, the local stress $\underset{\sim}{\sigma}^g$ is expressed according to global stress $\underset{\sim}{\sigma}$, the global strain $\underset{\sim}{\varepsilon}$ and the local strain $\underset{\sim}{\varepsilon}^g$:

$$\dot{\underset{\sim}{\sigma}}^g = \dot{\underset{\sim}{\sigma}} + \underset{\sim}{\underset{\sim}{\mathbf{L}}}^* \left(\dot{\underset{\sim}{\varepsilon}} - \dot{\underset{\sim}{\varepsilon}}^g\right) \tag{16}$$

The fourth order tensor $\underset{\sim}{\underset{\sim}{\mathbf{L}}}^*$ takes into account the incremental behavior of the equivalent medium and the tangent behavior of each grain. (Berveiller and Zaoui, 1979) proposed an explicit transition rule using the approximation of global isotropy, for a radial monotonic loading path:

$$\underset{\sim}{\sigma}^g = \underset{\sim}{\sigma} + \mu\alpha \left(\underset{\sim}{\sigma}, \underset{\sim}{\mathbf{E}}^p\right) \left(\underset{\sim}{\mathbf{E}}^p - \underset{\sim}{\varepsilon}^g\right) \quad \text{with} \quad \frac{1}{\alpha} \simeq 1 + \frac{3\mu E^p}{2\Sigma} \tag{17}$$

where Σ and E^p are respectively the overall equivalent stress and the plastic part of overall strain in uni-axial tension test. They showed also that Eq. 17 allows plastic accommodation in the polycrystal, meanwhile Kröner's rule (obtained with $\alpha = 1$ (Kröner, 1961)) produces only elastic elastic accommodation and too large stresses. The idea behind all the approaches is finally to introduce a corrective term depending on plastic strains, to compute local residual stresses. Nevertheless, a linear dependency of this

term with respect to plastic strains gives too large stresses. This concept was then replaced by (Cailletaud, 1987), (Cailletaud and Pilvin, 1994) and (Pilvin, 1996), who proposed a "β_rule" model in which the local strain is replaced by a phenomenological variable $\underset{\sim}{\beta}^g$. This new variable was shown able to correctly capture the plastic accommodation which comes from the self consistent formalism. When applied to material presenting isochoric plastic flow and uniform isotropic elasticity with a macroscopic shear modulus μ, the expression of the local stress $\underset{\sim}{\sigma}^g$ is:

$$\underset{\sim}{\sigma}^g = \underset{\sim}{\sigma} + \mu \left(\underset{\sim}{\beta} - \underset{\sim}{\beta}^g \right) \quad \text{with} \quad \underset{\sim}{\beta} = \left\langle \underset{\sim}{\beta}^g \right\rangle \tag{18}$$

The symbol $\langle . \rangle$ denotes the volume average. The variable $\underset{\sim}{\beta}^g$ presents a nonlinear evolution with respect to plastic strain:

$$\dot{\underset{\sim}{\boldsymbol{\beta}}}^g = \dot{\underset{\sim}{\boldsymbol{\varepsilon}}}^g - D \underset{\sim}{\boldsymbol{\beta}}^g ||\dot{\varepsilon}^g|| \tag{19}$$

This formulation is purely explicit; it does not need any iterative procedure like for classical self consistent model. The parameter D is a scale transition parameter, which should be fitted by means of Finite Element computations on realistic polycrystalline aggregates.

2.2 Application for two mechanisms

According to Kröner, the physical idea behind the self-consistent framework is the assumption of perfect disorder. It means that the mixture of the two constituents is such that in a given realization, the probability to find phase A and phase B in a given place is totally random. As a consequence, phase A can be seen as an inclusion in the homogeneous equivalent medium made of A and B, and phase B can also be seen as an inclusion in the homogeneous

equivalent medium made of A and B. This is why the localization rules for both phases are totally symmetric. The "β_rule" is selected for its simplicity and its versatility. It is now applied to the case of a 2-phase materials. The role played by its parameters will be studied, and the capabilities of the new models will be discussed. A similar localization process that is incorporated into 2M1C and 2M2C models have, as a common root, a decomposition of the total strain into an elastic part and two inelastic ones. Each inelastic strain can be associated with a particular mechanism I ($I = 1$ for the first mechanism and $I = 2$ for the second mechanism). The total inelastic strain $\underset{\sim}{\varepsilon}_{in}$ is the average of the irreversible deformation of each mechanism:

$$\underset{\sim}{\varepsilon}^{in} = (1 - z)\underset{\sim}{\varepsilon}^{1} + z\underset{\sim}{\varepsilon}^{2} \tag{20}$$

where $(1-z)$ and z are the volume fraction attributed to the first and the second mechanism respectively. The multi-mechanism approach is intended to describe the contribution of several physical levels, or deformation mechanism, to the inelastic behavior. For the application to the transformation induced plasticity (Gautier and Cailletaud, 2004), (Sai et al., 2006b), the volume fraction of each phase is calculated by a kinetics transformation rule. For the specific case of 316 stainless steel, the volume fraction z can be estimated with the help of the optimization process. The obtained value of the parameter z indicates the influence of each physical mechanism on the global behavior. The localization rule, simply writes:

$$\underset{\sim}{\sigma}^{1} = \underset{\sim}{\sigma} + \mu' \left(\underset{\sim}{\beta} - \underset{\sim}{\beta}^{1}\right) \quad \underset{\sim}{\sigma}^{2} = \underset{\sim}{\sigma} + \mu' \left(\underset{\sim}{\beta} - \underset{\sim}{\beta}^{2}\right) \tag{21}$$

with:

$$\underset{\sim}{\beta} = (1 - z)\underset{\sim}{\beta}^{1} + z\underset{\sim}{\beta}^{2} \tag{22}$$

The modified models are respectively called 2M1C_β and 2M2C_β. The new interphase accommodation variables $\underset{\sim}{\beta}^I$ are defined by:

$$\dot{\underset{\sim}{\boldsymbol{\beta}}}^I = \dot{\underset{\approx}{\boldsymbol{\varepsilon}}}^I - d_I \underset{\sim}{\boldsymbol{\beta}}^I ||\dot{\varepsilon}^I|| \tag{23}$$

2.3 Improvement of the kinematic hardening rule for each mechanism

The previous versions of the model used a classical version of the non linear kinematic rule, as expressed by Eq. 10 (Cailletaud and Sai, 1995), (Contesti and Cailletaud, 1989). This rule may become more versatile for the description of ratchetting by changing the direction of the fading memory term (Burlet and Cailletaud, 1987):

$$\begin{cases} \underset{\approx}{\mathbf{X}} = \delta \underset{\approx}{\mathbf{X}}^1 + (1-\delta)\underset{\approx}{\mathbf{X}}^2 \qquad \underset{\approx}{\mathbf{X}}^1 = \frac{2}{3} C \underset{\approx}{\alpha}^1 \qquad \underset{\approx}{\mathbf{X}}^2 = \frac{2}{3} C \underset{\approx}{\alpha}^2 \\ \dot{\underset{\approx}{\alpha}}^1 = \dot{\lambda}\left(\underset{\approx}{\mathbf{n}} - \frac{3D}{2C}\left(\underset{\approx}{\mathbf{X}} : \underset{\approx}{\mathbf{n}}\right) : \underset{\approx}{\mathbf{n}}\right) \quad \text{and} \quad \dot{\underset{\approx}{\alpha}}^2 = \dot{\lambda}\left(\underset{\approx}{\mathbf{n}} - \frac{3D}{2C}\underset{\approx}{\mathbf{X}}\right) \end{cases} \tag{24}$$

The original version of the model involves 2 kinematic hardening variables with two different fading memory terms using only one set of parameters (C, D). Other authors (Delobelle et al., 1995) have used a different combination of the same terms:

$$\begin{cases} \underset{\approx}{\mathbf{X}} = \underset{\approx}{\mathbf{X}}^1 + \underset{\approx}{\mathbf{X}}^2 \qquad \underset{\approx}{\mathbf{X}}^1 = \frac{2}{3} C \underset{\approx}{\alpha}^1 \qquad \underset{\approx}{\mathbf{X}}^2 = \frac{2}{3} C \underset{\approx}{\alpha}^2 \\ \dot{\underset{\approx}{\alpha}}^I = \dot{\lambda}\left(\underset{\approx}{\mathbf{n}} - \frac{3D_I}{2C_I}\left((1-\delta)\underset{\approx}{\mathbf{X}}^I + \delta\left(\underset{\approx}{\mathbf{X}}^I : \underset{\approx}{\mathbf{n}}^I\right)\underset{\approx}{\mathbf{n}}^I\right)\right) \quad (I = 1,2) \end{cases} \tag{25}$$

In the present paper, the following rule will be used:

$$\dot{\underset{\approx}{\alpha}}^I = \dot{\lambda}\left(\underset{\approx}{\mathbf{n}}^I - \frac{3D_I}{2C_{II}}\left((1-\delta_I)\underset{\approx}{\mathbf{X}}^I + \delta_I\left(\underset{\approx}{\mathbf{X}}^I : \underset{\approx}{\mathbf{n}}^I\right)\underset{\approx}{\mathbf{n}}^I\right)\right) \quad (I = 1,2) \tag{26}$$

where δ_I ($I = 1, 2$) are two additive material parameters. It is important to note that, from a thermodynamical point of view, the fading memory terms have to

be written as function of the back stresses $\underset{\sim}{\mathbf{X}}^I$ instead of the internal variables $\underset{\sim}{\alpha}^I$. This difference vanishes for unified models in isothermal conditions. 2M2C_β and 2M1C_β models (Table 3 and Table 4) are implemented into the Finite Element code ZéBuLoN (Besson et al., 1998), using a θ–method solved by an implicit Newton scheme for the local integration. In the next section, the simulations of the tests with the two modified models are shown.

3 New capabilities of the model

The purpose of this section is to illustrate the capabilities of the new models to describe specific mechanical effects. The two examples are treated with the 2M1C_β model; for the ratchetting effect, the same results would be obtained with the 2M2C_β model.

3.1 Ratchetting effect

In the new models, the effective stresses for each mechanism can be rewritten as $\underset{\sim}{\sigma} - \underset{\sim}{\mathbf{Y}}^I$, with:

$$\begin{pmatrix} \underset{\sim}{\mathbf{Y}}^1 \\ \\ \underset{\sim}{\mathbf{Y}}^2 \end{pmatrix} = \frac{2}{3} \begin{pmatrix} C_{11} & C_{12} \\ \\ C_{12} & C_{22} \end{pmatrix} \begin{pmatrix} \underset{\sim}{\alpha}^1 \\ \\ \underset{\sim}{\alpha}^2 \end{pmatrix} + \mu' \begin{pmatrix} z & -z \\ \\ -(1-z) & (1-z) \end{pmatrix} \begin{pmatrix} \underset{\sim}{\beta}^1 \\ \\ \underset{\sim}{\beta}^2 \end{pmatrix}$$

This illustrates the difference between the intermechanism and intramechanism corrective terms for computing internal stresses. When both $\underset{\sim}{\beta}^I$ and $\underset{\sim}{\mathbf{X}}^I$ have linear evolution rules, it can be easily shown that the modified models are reduced to the initial form with the following determinant of the hardening

matrix:

$$\Delta = (4/9)(C_{11}C_{22} - C_{12}^2) + (2/3)\mu' \left[(1-z)C_{11} + zC_{22} + C_{12}\right]$$

As a consequence, ratchetting behavior depends both on the initial determinant $C_{11}C_{22} - C_{12}^2$ and the localization parameter μ'. A systematic study is then proposed to illustrate the uniaxial and the multi-axial ratchetting behavior with respect to (i) the evolution rule of the accommodation variables $\underset{\sim}{\beta}^I$, (ii) the evolution rule of the back stresses $\underset{\sim}{\mathbf{X}}^I$, and (iii) the characteristics of the hardening matrix $[\mathbf{C}]$. In order to easily identify the various tests, their names are defined by five letters. The first one characterizes the regular (R)/ singular (S) matrix. The next two capital letters are allotted to the description of the kinematic hardening evolution rules (L for linear and N for non linear hardening rules). The last two small letters are reserved to the description of the evolution rules of the accommodation variables (l for linear and n for non linear). For example:

- the model with a singular matrix, linear evolution rules for the kinematic variables and linear evolution rules for the accommodation variables will be refered to as model SLLll,
- the model with a regular matrix, linear evolution rule for the first kinematic variable, non linear evolution rule for the second kinematic variable and non linear evolution rules for the accommodation variables will be refered to as model RLNnn.

The list of the parameters used for each model is given in Table 5, and the corresponding predicted uniaxial ratchetting response for applied stresses are shown in Fig. 3. The main results can be summarized as follows:

- Ratchetting behavior with a constant increase of a tensile peak strain is obtained in the following cases:
  - · for a singular matrix ($\Delta = 0$) and linear evolution rules for both kinematic hardening variables whatever the evolution rules of the accommodation variables (models SLLll and SLLnn),
  - · for a regular matrix ($\Delta \neq 0$) and non linear evolution rules for the two kinematic hardening variables and the two accommodation variables (model RNNnn),
- Ratchetting behavior also occurs but with a lower rate with a regular matrix, two linear kinematic hardening variables and two non linear accommodation variables (RLLnn)
- A shakedown behavior is obtained with a regular matrix if one (at least) of the kinematic hardening variables is linear and one (at least) of the the accommodation variables is linear (models RLLll, RNLll, RLLnl).
- Ratchetting can also be stopped with two non linear kinematic variables if a regular matrix and two linear accommodation variables are used (model RNNll). However, the asymptotic tensile peak strain reached at steady state is large by comparison with the models RLLll, RNLll, RLLnl.

3.2 Behavior under nonproportional loading

In combined axial-torsional fatigue tests, "out-of-phase" tests refer to sinusoïdal signals with a 90°phase lag, meanwhile for "in-phase" loadings, the phase lag is zero. A material exhibits an "additional hardening" if the equivalent stress range obtained in "out-of-phase" test is larger than those obtained for any "in-phase" test having the same equivalent strain range.

Materials like austenitic stainless steel or copper are famous to be prone to additional hardening (Cailletaud et al., 1984), (Lamba and Sidebottom, 1978), (Benallal and Marquis, 1987). Surprisingly, the 2M1C Model can reproduce this additional hardening. To illustrate this possibility, an axial fatigue test with a strain range of 1% is compared to a tension-torsion out-of-phase test with the same axial strain range. As shown in Fig. 4, the resulting stress range is larger for the out-of-phase test than for the axial test. Note that the model has not specific material constants to describe the degree of additional hardening. It will be shown in the next section that the 2M1C_β model is able to predict with a good accuracy the amount of additional hardening obtained for experiments. On the other hand, it is worth noting that this extra-hardening has a pure kinematic source, so that it will vanish after one or two cycles in an "in-phase" loading which would follow an "out-of-phase" block. This is not the case in the experiments when the memory of the initial extra-hardening will slowly vanish in the subsequent loading.

4 Application to 316 stainless steel at 25°C

In many cases, the local deformation mechanisms that produce plasticity in metallic materials generate heterogeneous deformation patterns. This is the fundamental reason for introducing several mechanisms. Two mechanisms is the preferred version, since it provides a series of interesting modeling capabilities, even if they are still manageable. For the specific case of 316 stainless steel, dislocation patterns are known to be present in the grains. Their form can be either walls or cells according to the level of the loading and its type. The set dislocation walls / interwall areas can be seen as the physical

reason for the two mechanisms in the present case.

4.1 Results of simulation of experiments

To assess the models capabilities to quantitatively describe the experimental effects, an experimental data base obtained on a 316 stainless steel is chosen (Portier et al., 2000). As in the cited work, the following tests at room temperature (25°C) have been used for the identification of the modified 2M1C and 2M2C models:

- monotonic tensile test,
- cyclic uni-axial tension-compression for three strain ranges,
- tension-torsion ratchetting tests with two values of tensile stress and with various shear strain amplitude,
- tension-torsion out-of-phase test at mechanical steady-state.

The loading histories related to the different simulations are shown in Fig. 5. The materials parameter identification was performed by means of the optimization module of the software Zset/Zébulon. To reduce the number of parameters in the identification procedure, the evolution rules of the accommodation variables are taken linear for the two models. For the 2M2C_β model one kinematic hardening variable was taken as quasi-linear to reduce ratchet strain which is much too large with two nonlinear kinematic variables. The list of the calibrated coefficients for the 2M1C_β and the 2M2C_β models is given in Tables 6 and 7, and the corresponding comparison between simulated responses and experimental data are shown in Fig. 6. According to Table 7, only the second mechanism in the 2M2C_β model has isotropic hardening. This is in agreement with the fact that there is a soft phase (the areas with

a low dislocation density) and a hard phase (dislocation walls or cells). The harder phase is also the phase which will become harder and harder during the deformation process. For sure, this has an influence on the description of ratchetting. In addition to the tension ratchetting test which is not included in the identification procedure, two tension-torsion ratchetting tests are used to validate a posteriori the prediction of the proposed model (Fig. 7). In these tests, the specimens are submitted to a constant axial strain with an increasing shear strain amplitude. The correlation between simulated responses and experimental results for the optimal set of material parameters are globally satisfactory. In fact:

- the 2M1C_β model does not reproduce each tension-torsion ratchetting test exactly but it is able to capture the major trends in the tests. In particular, the out-of-phase test is well described by this model.
- the 2M2C_β model gives a more precise description of the 2D ratchetting tests but underestimates the additional hardening under nonproportional cyclic loading.

Comparing to the models tested in the work of (Portier et al., 2000), the proposed models are able to reproduce both ratchetting under uni-axial condition and multi-axial condition.

4.2 Discussion

The overestimation of the ratchetting by the 2M1C_β model and its underestimation by the 2M2C_β model is not a motivation to diversify the multi-mechanism models but rather to converge towards an unique formulation. The true nature of the two models was exhibited in Fig. 1, in

a conventional representation, in terms of effective stresses $(\underset{\sim}{\sigma} - \underset{\sim}{\mathbf{X}}^1, \underset{\sim}{\sigma} - \underset{\sim}{\mathbf{X}}^2)$. By the way, intermediate solutions can also be found, and, following (Gambin and Kröner, 1981), a non linear combination of the two mechanisms has already been proposed (Taleb et al., 2006):

$$f = \left[\left(\frac{J(\underset{\sim}{\sigma} - \underset{\sim}{\mathbf{X}}^1)}{K_1} \right)^N + \left(\frac{J(\underset{\sim}{\sigma} - \underset{\sim}{\mathbf{X}}^2)}{K_2} \right)^N \right]^{1/N} - R \tag{27}$$

where N is a new material parameter. 2M1C model is recovered by using $N = 2$, meanwhile 2M2C model is the limit case when $N \to \infty$. K_1 and K_2 are not new material parameters. They are equal for the 2M1C model. For the 2M2C model, K_1 and K_2 are related to the ratio of the initial yield surfaces R_1^0 and R_2^0. The effect of the new parameter N is shown on Fig. 8. For $N = 1$, the obtained curve is a rhomboid, for the $N = 2$ (2M1C model) it is a circle, while for $N \to \infty$ it is a rectangle (2M2C model).

The parameter set of Table 6 is used to simulate out-of-phase tests with various values of N (K_1=K_2=1). Figure 9 gives the resulting additional hardening for different values of N. It can be noted that:

- the additional hardening is absent for very small values of the parameter N (say 1.1) and for the high values of N (corresponding to the 2M2C model),
- the maximum additional hardening is obtained with $N \simeq 3$,
- the optimum value that gives the more precise amount of additional hardening in the present case is N=2 (corresponding to the 2M1C model), or, alternatively for $N \simeq 4$.

In this unique formulation, chosing N=1 produces a version which may degenerate into an unified model with two back stresses for some particular loadings. For instance, in one dimensional tensile loading, the yield function of

Eq. 27 is such that:

$$f = |\sigma - X^1| + |\sigma - X^2| - R = 2\sigma - X^1 - X^2 - R \tag{28}$$

On the other hand, taking a yield function as in Eq. 27 does not preserve the opportunity to introduce two different mechanisms, (namely viscoplastic and plastic) in the constitutive equations. Further simulations are needed to explore the effect of the parameter N on the description of the whole range of experimental data.

5 Conclusion

This paper shows the current state of a class of multi-mechanism models with either unified or additive (visco)plastic flows. It was established from previous works that, for this type of models, ratchetting behavior is related to the value of the determinant of the hardening matrix. The improvement proposed here takes its source in the β_rule (Cailletaud and Pilvin, 1994) already used in polycrystalline approches and from an alternative formulation of the kinematic hardening rule (Burlet and Cailletaud, 1987). As a result, a good agreement is obtained between the proposed model and an experimental data base consisting of one dimensional and multi-axial tests. These results do not imply that the proposed models are general enough for simulating successfully the ratchetting in an other experimental data base. Further validation are needed to explore their general reliability.

The proposed 2M1C_β and 2M2C_β models are characterized by a high versatility with regard to ratchetting behavior. Fully equipped with singular and regular/singular matrices and with different choices of fading memory

terms, they are implemented in the Finite Element code Zébulon; it is then possible to use them for structural computations, in order to analyze the inelastic behavior of machine components submitted to complex multi-axial loading.

References

Abdel-Karim, M. (2005). Numerical integration method for kinematic hardening rules with partial activation of dynamic recovery term. *Int. J. Plasticity*, 21:1303–1321.

Abdel-Karim, M. and Ohno, N. (2000). Kinematic hardening model suitable for ratchetting with steady-state. *Int. J. Plasticity*, 16:225–240.

Armstrong, P. and Frederick, C. (1966). A mathematical representation of the multiaxial Baushinger effect. In *G.E.C.B.* Report RD/B/N 731.

Bari, S. and Hassan, T. (2000). Anatomy of coupled constitutive models for ratcheting simulation. *Int. J. Plasticity*, 16:381–409.

Bari, S. and Hassan, T. (2001). Kinematic hardening rules in uncoupled modeling for multiaxial ratcheting simulation. *Int. J. Plasticity*, 17:885–905.

Bari, S. and Hassan, T. (2002). An advancement in cyclic plasticity modeling for multiaxial ratcheting simulation. *Int. J. Plasticity*, 18:873–894.

Basuroychowdhury, I. N. and Voyiadjis, G. Z. (1998). A multiaxial cyclic plasticity model for non-proportional loading cases. *Int. J. Plasticity*, 14:855–870.

Benallal, A. and Marquis, D. (1987). Constitutive equations for nonproportional cyclic elasto-viscoplasticity. *ASME J. Engng. Mater. Techn.*, 109:326–336.

Berveiller, M. and Zaoui, A. (1979). An extension of the self-consistent scheme to plastically-following polycrystals. *J. Mech. Phys. Solids*, 26:325–344.

Besson, J., Leriche, R., Foerch, R., and Cailletaud, G. (1998). Object-oriented programming applied to the finite element method. Part II. application to material behaviors. *Revue Européenne des Eléments finis*, 7:567–588.

Bocher, L., Delobelle, P., Robinet, P., and Feaugas, X. (2001). Mechanical and microstructural investigations of an austenitic stainless steel under non-proportional loadings in tension-torsion-internal and external pressure. *Int. J. Plasticity*, 17:1491–1530.

Burlet, H. and Cailletaud, G. (1987). Modelling of cyclic plasticity in finite element codes. In *Proc. of 2nd Int. Conf. on Constitutive laws for Engineering Materials; Theory and Application*. Tucson, AZ.

Cailletaud, G. (1987). *Une approche micromécanique phénoménologique du comportement inélastique des métaux*. PhD thesis, Université Pierre et Marie Curie, Paris 6.

Cailletaud, G. (1992). A micromechanical approach to inelastic behaviour of metals. *Int. J. Plasticity*, 8:55–73.

Cailletaud, G., Kaczmarek, H., and Policella, H. (1984). Some elements on multiaxial behavior of 316 stainless steel at room temperature. *Mech. Mat.*, 3:333–347.

Cailletaud, G. and Pilvin, P. (1994). Utilisation de modèles polycristallins pour le calcul par éléments finis. *Revue Européenne des Eléments Finis*, 3:515–541.

Cailletaud, G. and Sai, K. (1995). Study of plastic/viscoplastic models with various inelastic mechanisms. *Int. J. Plasticity*, 11:991–1005.

Chaboche, J. (1986). Time-independent constitutive theories for cyclic plasticity. *Int. J. Plasticity*, 2:149–188.

Chaboche, J. and Jung, O. (1997). Application of a kinematic hardening viscoplasticity model with threshold to the residual stress relaxation. *Int. J. Plasticity*, 13:785–807.

Chaboche, J., Nouailhas, D., Pacou, D., and Paulmier, P. (1991). Modeling of the cyclic response and ratchetting effect on inconel 718 alloy. *Eur. J. Mech. Solids*, 10:101–121.

Chaboche, J. and Rousselier, G. On the plastic and viscoplastic constitutive equations, Part II.

Contesti, E. and Cailletaud, G. (1989). Description of creep plasticity interaction with non unified constitutive equations : application to an austenitic stainless steel. *Nuclear Eng. and Design*, 116:265–280.

Dafalias, Y. and Popov, E. (1976). Plastic internal variables formalism of cyclic plasticity. *ASME J. of Appl. Mech.*, 43:645–651.

Delobelle, P., Robinet, P., and Bocher, L. (1995). Experimental study and phenomenological modelization of ratchet under uniaxial and biaxial loading on an austenitic stainless steel. *Int. J. Plasticity*, 11:295–330.

Feaugas, X. and Gaudin, C. (2004). Ratchetting process in the stainless steel aisi 316L at 300 K: an experimental investigation. *Int. J. Plasticity*, 20:643–662.

Gambin, B. and Kröner, E. (1981). Convergence problems in the theory of random elastic media. *Int. J. of Eng. Sci.*, 19:313–318.

Gautier, E. and Cailletaud, C. (2004). N-phase modeling applied to phase transformations in steels: a coupled kinetics-mechanics approach. In *ICHMM-2004 Internationnal Conference on Heterogeneous Material Mechanics*. Chongqing (Chine).

Germain, P., Nguyen, Q., and Suquet, P. (1983). Continuum thermodynamics. *J. Appl. Mech.*, 50:1010–1020.

Halphen, B. and Nguyen, Q. (1975). Sur les matériaux standards généralisés. *J. Mécanique*, 14:39–63.

Hassan, T., Corona, E., and Kyriakides, S. (1992a). Ratcheting in cyclic plasticity, Part II: Multiaxial behavior. *Int. J. Plasticity*, 8:117–146.

Hassan, T., Corona, Y., and Kyriakides, S. (1992b). Ratcheting in cyclic plasticity, Part I: Uniaxial behavior. *Int. J. Plasticity*, 8:91–116.

Hassan, T. and Kyriakides, S. (1994a). Ratcheting of cyclically hardening and softening materials, Part I uniaxial behavior. *Int. J. Plasticity*, 10:149–184.

Hassan, T. and Kyriakides, S. (1994b). Ratcheting of cyclically hardening and softening materials, Part II multiaxial behavior. *Int. J. Plasticity*, 10:185–212.

Hill, R. (1965). Continuum micro-mechanisms of elastoplastic polycrystals. *J. Mech. Phys. Solids*, 13:89–101.

Jiang, Y. and Kurath, P. (1996). Characteristics of the Armstrong-Frederick type plasticity models. *Int. J. Plasticity*, 12:387–415.

Jiang, Y. and Sehitoglu, H. (1994a). Cyclic ratchetting of 1070 steel under multiaxial stress states. *Int. J. Plasticity*, 10:579–608.

Jiang, Y. and Sehitoglu, H. (1994b). Multiaxial cyclic ratchetting under multiple step loading. *Int. J. Plasticity*, 8:849–870.

Kang, G., Gao, Q., and Yang, X. (2002). Uniaxial cyclic ratchetting and plastic flow properties of SS304 stainless steel at room and elevated temperatures. *Mech. Mat.*, 34:145–159.

Kang, G., Kan, Q., Zhang, J., and Sun, Y. (2006). Time-dependent ratchetting experiments of SS304 stainless steel. *Int. J. Plasticity*, 22:858–894.

Khabou, T., Castex, L., and Inglebert, G. (1990). The effect of material behavior law on the theoretical shot peening results. *Eur. J. Mech.*

A/Solids, 9:537–549.

Krieg, R. (1975). A practical two-surface plasticity theory. *Tans. ASME*, 45:641–646.

Kröner, E. (1961). Zur plastischen Verformung des Vielkristalls. *Acta Metall.*, 9:155–161.

Lamba, H. and Sidebottom, O. (1978). Cyclic plasticity for nonproportional paths, Parts I and II. *ASME J. Engng. Mater. Techn.*, 100:96–111.

McDowell, D. L. (1995). Stress state dependence of cyclic ratchetting behavior of two rail steels. *Int. J. Plasticity*, 11:397–421.

Mizunno, M., Mima, Y., Abdel-Karim, M., and Ohno, N. (2000). Uniaxial ratchetting of 316FR steel at room temperature, Part I. *J. of Engng. Mat. and Tech.*, 122:29–33.

Molinari, A. (1999). Extensions of the self-consistent tangent model. *Modelling Simul. Mater. Sci. Eng.*, 7:683–697.

Mroz, Z. (1967). On the description of anisotropic work-hardening. *J. Mech. Phys. Sol.*, 15:163–175.

Ohno, N., Abdel-Karim, M., Kobayashi, M., and Igari, T. (1998). Ratchetting characteristics of 316FR steel at high temperature, Part I: Strain-controlled ratchetting experiments and simulations. *Int. J. Plasticity*, 14:355–372.

Ohno, N. and Wang, J. (1993a). Kinematic hardening rules with critical state for activation of dynamic recovery, Part II: application to experiments of ratchetting behaviour. *Int. J. Plasticity*, 9:391–403.

Ohno, N. and Wang, J. (1993b). Kinematic hardening rules with critical state of dynamic recovery, Part I: formulation and basis features for ratchetting behaviour. *Int. J. Plasticity*, 9:375–390.

Pilvin, P. (1996). The contribution of micromechanical approaches to

the modelling of inelastic behaviour of polycrystals. In Pineau, A., Cailletaud, G., and Lindley, T., editors, *Fourth Int. Conf. on Biaxial/Multiaxial Fatigue and Design*. London ESIS 21, Mechanical Engineering Publications.

Portier, L., Calloch, S., Marquis, D., and Geyer, P. (2000). Ratchetting under tension-torsion loading: experiments and modelling. *Int. J. Plasticity*, 16:303–335.

Ristinmaa, M. (1995). Cyclic plasticity model using one yield surface only. *Int. J. Plasticity*, 11:163–181.

Ruggles, M. and Krempl, E. (1989). The influence of the test temperature on the ratchetting behavior of type 304 stainless steel. *ASME J. Engng. Mat. and Techn.*, 111:378–383.

Sai, K., Aubourg, V., Cailletaud, G., and Strudel, J. (2004). Physical basis for model with various inelastic mechanisms for nickel base superalloy. *Materials Science and Technology*, 20:747–755.

Sai, K., Cailletaud, G., and Forest, S. (2006a). Micro-mechanical modeling of the inelastic behavior of directionally solidified materials. *Mechanics of Materials*, 38:203–217.

Sai, K., Cailletaud, G., Tourki, Z., Gautier, E., and Amor, A. (2006b). N-phase modeling of phase transformation in 304 stainless steel, bulging: Finite element simulation and experimental validation. In *12^{th} International Symposium on Plasticity and its Applications*. Halifax, Nova Scotia, Canada 2006.

Taheri, S. and Lorentz, E. (1999). An elasto-plastic constitutive constitutive law for the description of uniaxial and multiaxial ratchetting. *Int. J. Plasticity*, 15:1159–1180.

Taleb, L., Cailletaud, G., and Blaj, L. (2006). Numerical simulation of complex

ratcheting tests with a multi-mechanism model type. *Int. J. Plasticity*, 22:724–753.

Taylor, G. (1938). Plastic strain in metals. *J. Inst. Metals*, 62:307–324.

Videau, J., Cailletaud, G., and Pineau, A. (1994). Modélisation des effets mécaniques des transformations de phases. *J. de Phys.*, 4:227–232.

Vincent, L., Calloch, S., and Marquis, D. (2004). A general cyclic plasticity model taking into account yield surface distortion for multiaxial ratchetting. *Int. J. Plasticity*, 20:1817–1850.

Yaguchi, M. and Takahashi, Y. Ratchetting of viscoplastic material with cyclic softening, Part I: experiments on modified 9Cr-1Mo steel. *Int. J. Plasticity*, 21, pages = 43-65, year = 2005.

Yaguchi, M. and Takahashi, Y. (2005). Ratchetting of viscoplastic material with cyclic softening, Part II: application of constitutive models. *Int. J. Plasticity*, 21:835–860.

Yoshida, F. (1989). Rate dependent behaviour of 304 stainless steel under uniaxial creep-ratchetting and biaxial cyclic loading at room temperature. structural design for elevated temperature environments-creep ratchet, fatigue and fracture. *ASME Pressure Vessels and Piping Conference*, 163:81–86.

Yoshida, F. (2000). A constitutive model of cyclic plasticity. *Int. J. Plasticity*, 16:359–380.

Zarka, J. and Casier, J. (1979). Elastic plastic response of structure to cyclic loading. In *Mechanics today Vol. 6*. ed. Nemat-Nasser (Pergamon Press, New York).

Zarka, J. and Navidi, P. (1998). Intelligent modeling of materials. *Mechanics of Materials*, 28:61–82.

List of Tables

List of Figures

6 Tables

Table 1

Constitutive equations of the initial 2M2C model

$$\dot{\underset{\sim}{\varepsilon}} = \dot{\underset{\sim}{\varepsilon}}^e + \dot{\underset{\sim}{\varepsilon}}^1 + \dot{\underset{\sim}{\varepsilon}}^2$$

$$f^1 = J(\underset{\sim}{\sigma} - \underset{\sim}{\mathbf{X}}^1) - R^1 - R_0^1 \qquad f^2 = J(\underset{\sim}{\sigma} - \underset{\sim}{\mathbf{X}}^2) - R^2 - R_0^2$$

$$\begin{pmatrix} \underset{\sim}{\mathbf{X}}^1 \\ \\ \underset{\sim}{\mathbf{X}}^2 \end{pmatrix} = (2/3) \begin{pmatrix} C_{11}\ C_{12} \\ \\ C_{12}\ C_{22} \end{pmatrix} \begin{pmatrix} \underset{\sim}{\alpha}^1 \\ \\ \underset{\sim}{\alpha}^2 \end{pmatrix}$$

$$R^1 = Q_1 r^1 \qquad R^2 = Q_2 r^2$$

$$\dot{\underset{\sim}{\varepsilon}}^1 = \dot{\lambda}^1 \underset{\sim}{\mathbf{n}}^1 \qquad \dot{\underset{\sim}{\varepsilon}}^2 = \dot{\lambda}^2 \underset{\sim}{\mathbf{n}}^2$$

$$\dot{\underset{\sim}{\alpha}}^1 = \dot{\lambda}^1 \left(\underset{\sim}{\mathbf{n}}^1 - \frac{3D_1 \underset{\sim}{\mathbf{X}}^1}{2C_{11}} \right) \qquad \dot{\underset{\sim}{\alpha}}^2 = \dot{\lambda}^2 \left(\underset{\sim}{\mathbf{n}}^2 - \frac{3D_2 \underset{\sim}{\mathbf{X}}^2}{2C_{22}} \right)$$

$$\dot{r}^1 = \dot{\lambda}^1 \left(1 - \frac{b_1 R^1}{Q_1} \right) \qquad \dot{r}^2 = \dot{\lambda}^2 \left(1 - \frac{b_2 R^2}{Q_2} \right)$$

Table 2

Constitutive equations of the initial 2M1C model

$$\dot{\underset{\sim}{\varepsilon}} = \dot{\underset{\sim}{\varepsilon}}^{e} + \dot{\underset{\sim}{\varepsilon}}^{1} + \dot{\underset{\sim}{\varepsilon}}^{2}$$

$$f = \left(J(\underset{\sim}{\sigma} - \underset{\sim}{\mathbf{X}}^{1})^2 + J(\underset{\sim}{\sigma} - \underset{\sim}{\mathbf{X}}^{2})^2\right)^{1/2} - R - R_0$$

$$\begin{pmatrix} \underset{\sim}{\mathbf{X}}^{1} \\ \\ \underset{\sim}{\mathbf{X}}^{2} \end{pmatrix} = (2/3) \begin{pmatrix} C_{11}\ C_{12} \\ \\ C_{12}\ C_{22} \end{pmatrix} \begin{pmatrix} \underset{\sim}{\alpha}^{1} \\ \\ \underset{\sim}{\alpha}^{2} \end{pmatrix}$$

$$R = Qr$$

$$\dot{\underset{\sim}{\varepsilon}}^{1} = \dot{\lambda}\underset{\sim}{\mathbf{n}}^{1} \qquad \dot{\underset{\sim}{\varepsilon}}^{2} = \dot{\lambda}\underset{\sim}{\mathbf{n}}^{2}$$

$$\dot{\underset{\sim}{\alpha}}^{1} = \dot{\lambda^{1}}\left(\underset{\sim}{\mathbf{n}}^{1} - \frac{3D_1\underset{\sim}{\mathbf{X}}^{1}}{2C_{11}}\right) \qquad \dot{\underset{\sim}{\alpha}}^{2} = \dot{\lambda^{2}}\left(\underset{\sim}{\mathbf{n}}^{2} - \frac{3D_2\underset{\sim}{\mathbf{X}}^{2}}{2C_{22}}\right)$$

$$\dot{r} = \dot{\lambda}\left(1 - \frac{bR}{Q}\right)$$

Table 3. Constitutive equations of the modified 2M2C model

$$\dot{\underset{\sim}{\varepsilon}} = \dot{\underset{\sim}{\varepsilon}}^e + (1-z)\dot{\underset{\sim}{\varepsilon}}^1 + z\dot{\underset{\sim}{\varepsilon}}^2$$

$$f^1 = J(\underset{\sim}{\sigma}^1 - \underset{\sim}{\mathbf{X}}^1) - R^1 - R_0^1 \qquad f^2 = J(\underset{\sim}{\sigma}^2 - \underset{\sim}{\mathbf{X}}^2) - R^2 - R_0^2$$

$$\underset{\sim}{\sigma}^1 = \underset{\sim}{\sigma} + \mu' \left(\underset{\sim}{\beta} - \underset{\sim}{\beta}^1\right) \qquad \underset{\sim}{\sigma}^2 = \underset{\sim}{\sigma} + \mu' \left(\underset{\sim}{\beta} - \underset{\sim}{\beta}^2\right)$$

$$\underset{\sim}{\beta} = (1-z)\underset{\sim}{\beta}^1 + z\underset{\sim}{\beta}^2$$

$$\begin{pmatrix} \underset{\sim}{\mathbf{X}}^1 \\ \\ \underset{\sim}{\mathbf{X}}^2 \end{pmatrix} = (2/3) \begin{pmatrix} C_{11}\ C_{12} \\ \\ C_{12}\ C_{22} \end{pmatrix} \begin{pmatrix} \underset{\sim}{\alpha}^1 \\ \\ \underset{\sim}{\alpha}^2 \end{pmatrix}$$

$$R^1 = Q_1 r^1 \qquad R^2 = Q_2 r^2$$

$$\dot{\underset{\sim}{\varepsilon}}^1 = \dot{\lambda}^1 \underset{\sim}{\mathbf{n}}^1 \qquad \dot{\underset{\sim}{\varepsilon}}^2 = \dot{\lambda}^2 \underset{\sim}{\mathbf{n}}^2$$

$$\dot{\underset{\sim}{\boldsymbol{\beta}}}^1 = \dot{\underset{\sim}{\boldsymbol{\varepsilon}}}^1 - d_1 \underset{\sim}{\boldsymbol{\beta}}^1 ||\dot{\varepsilon}^1|| \qquad \dot{\underset{\sim}{\boldsymbol{\beta}}}^2 = \dot{\underset{\sim}{\boldsymbol{\varepsilon}}}^2 - d_2 \underset{\sim}{\boldsymbol{\beta}}^2 ||\dot{\varepsilon}^2||$$

$$\dot{\underset{\sim}{\alpha}}^1 = \dot{\lambda} \left(\underset{\sim}{\mathbf{n}}^1 - \frac{3D_1}{2C_{11}} \left((1-\delta_1)\underset{\sim}{\mathbf{X}}^1 + \delta_1 \left(\underset{\sim}{\mathbf{X}}^1 : \underset{\sim}{\mathbf{n}}^1\right) \underset{\sim}{\mathbf{n}}^1\right)\right) \qquad \dot{\underset{\sim}{\alpha}}^2 = \dot{\lambda} \left(\underset{\sim}{\mathbf{n}}^2 - \frac{3D_2}{2C_{22}} \left((1-\delta_2)\underset{\sim}{\mathbf{X}}^2 + \delta_2 \left(\underset{\sim}{\mathbf{X}}^2 : \underset{\sim}{\mathbf{n}}^2\right) \underset{\sim}{\mathbf{n}}^2\right)\right)$$

$$\dot{r}^1 = \dot{\lambda}^1 \left(1 - \frac{b_1 R^1}{Q_1}\right) \qquad \dot{r}^2 = \dot{\lambda}^2 \left(1 - \frac{b_2 R^2}{Q_2}\right)$$

Table 4. Constitutive equations of the modified 2M1C model

$$\dot{\underset{\sim}{\varepsilon}} = \dot{\underset{\sim}{\varepsilon}}^{e} + (1-z)\dot{\underset{\sim}{\varepsilon}}^{1} + z\dot{\underset{\sim}{\varepsilon}}^{2}$$

$$f = \left(J(\underset{\sim}{\sigma}^{1} - \underset{\sim}{\mathbf{X}}^{1})^{2} + J(\underset{\sim}{\sigma}^{2} - \underset{\sim}{\mathbf{X}}^{2})^{2}\right)^{1/2} - R - R_0$$

$$\underset{\sim}{\sigma}^{1} = \underset{\sim}{\sigma} + \mu'\left(\underset{\sim}{\beta} - \underset{\sim}{\beta}^{1}\right) \qquad \underset{\sim}{\sigma}^{2} = \underset{\sim}{\sigma} + \mu'\left(\underset{\sim}{\beta} - \underset{\sim}{\beta}^{2}\right)$$

$$\underset{\sim}{\beta} = (1-z)\underset{\sim}{\beta}^{1} + z\underset{\sim}{\beta}^{2}$$

$$\begin{pmatrix} \underset{\sim}{\mathbf{X}}^{1} \\ \\ \underset{\sim}{\mathbf{X}}^{2} \end{pmatrix} = (2/3) \begin{pmatrix} C_{11}\ C_{12} \\ \\ C_{12}\ C_{22} \end{pmatrix} \begin{pmatrix} \underset{\sim}{\alpha}^{1} \\ \\ \underset{\sim}{\alpha}^{2} \end{pmatrix}$$

$$R = Qr$$

$$\dot{\underset{\sim}{\varepsilon}}^{1} = \dot{\lambda}\underset{\sim}{\mathbf{n}}^{1} \qquad \dot{\underset{\sim}{\varepsilon}}^{2} = \dot{\lambda}\underset{\sim}{\mathbf{n}}^{2}$$

$$\dot{\underset{\sim}{\boldsymbol{\beta}}}^{1} = \dot{\underset{\sim}{\boldsymbol{\varepsilon}}}^{1} - d_1\underset{\sim}{\boldsymbol{\beta}}^{1}||\dot{\varepsilon}^{1}|| \qquad \dot{\underset{\sim}{\boldsymbol{\beta}}}^{2} = \dot{\underset{\sim}{\boldsymbol{\varepsilon}}}^{2} - d_2\underset{\sim}{\boldsymbol{\beta}}^{2}||\dot{\varepsilon}^{2}||$$

$$\dot{\underset{\sim}{\alpha}}^{1} = \dot{\lambda}\left(\underset{\sim}{\mathbf{n}}^{1} - \frac{3D_1}{2C_{11}}\left((1-\delta_1)\underset{\sim}{\mathbf{X}}^{1} + \delta_1\left(\underset{\sim}{\mathbf{X}}^{1} : \underset{\sim}{\mathbf{n}}^{1}\right)\underset{\sim}{\mathbf{n}}^{1}\right)\right) \qquad \dot{\underset{\sim}{\alpha}}^{2} = \dot{\lambda}\left(\underset{\sim}{\mathbf{n}}^{2} - \frac{3D_2}{2C_{22}}\left((1-\delta_2)\underset{\sim}{\mathbf{X}}^{2} + \delta_2\left(\underset{\sim}{\mathbf{X}}^{2} : \underset{\sim}{\mathbf{n}}^{2}\right)\underset{\sim}{\mathbf{n}}^{2}\right)\right)$$

$$\dot{r} = \dot{\lambda}\left(1 - \frac{bR}{Q}\right)$$

Table 5

2M1C_β–Model, study of ratchetting behavior with respect to the different material parameters.

Coefficients	Model parameters								Units
	SLLll	RLLll	RLLnn	RLLln	SLLnn	RNNll	RNLll	RNNnn	
C_{11}	30	30	50	50	50	50	50	100	GPa
C_{22}	3	3	5	5	5	5	5	10	GPa
C_{12}	9.486	9.486	10	10	15.81	10	10	20	GPa
μ'	30	0	40	40	40	40	40	80	GPa
D_1	0	0	0	0	0	100	300	100	-
D_2	0	0	0	0	0	10	0	10	-
d_1	0	0	20	0	20	0	0	20	-
d_2	0	0	200	200	200	0	0	200	-

(z=0.79, R_0=250 MPa, Q=50 MPa, b=30)

Table 6

Identified material parameters of the 2M1C_β–Model. 316 austenitic stainless steel (25°C) E=192 GPa $\nu = 0.3$

R_0 = 163 MPa	Q = 129 MPa	b = =2.8	z=0.04	μ'=20 GPa
C_{11}=115.6 GPa	C_{22}=12.9 GPa	C_{12}=19.5 GPa	D_1=112.5	D_2=1464
δ_1=0.108	δ_2=0.0025	d_1=0	d_2=0	

Table 7

Identified material parameters of the 2M2C_β–Model. 316 austenitic stainless steel (25°C), E=192 GPa $\nu = 0.3$

R_0^1=145.6 MPa	Q_1=0 MPa	b_1=0			
R_0^2=220 MPa	Q_2 =200 MPa	b_2=4			
C_{11}=13 GPa	C_{22}=11 GPa	C_{12}=-7.3 GPa	D_1=0	D_2=388	
δ_1=0.038	δ_2=0.022	$d_1 = 0$	$d_2 = 0$	z=0.373	μ'=19.7 GPa

7 Figures

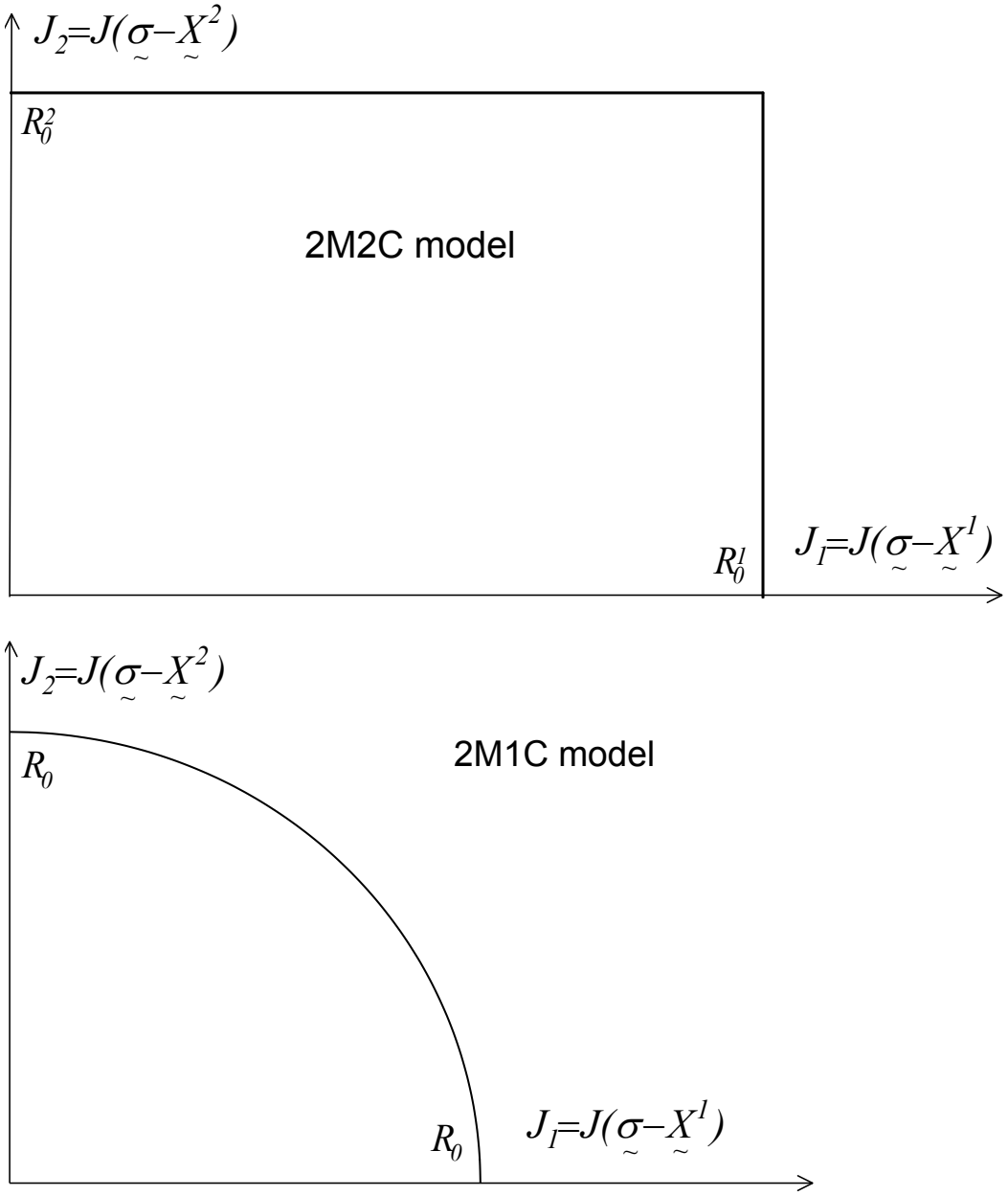

Fig. 1. Comparison of the initial elastic domain for the two models.

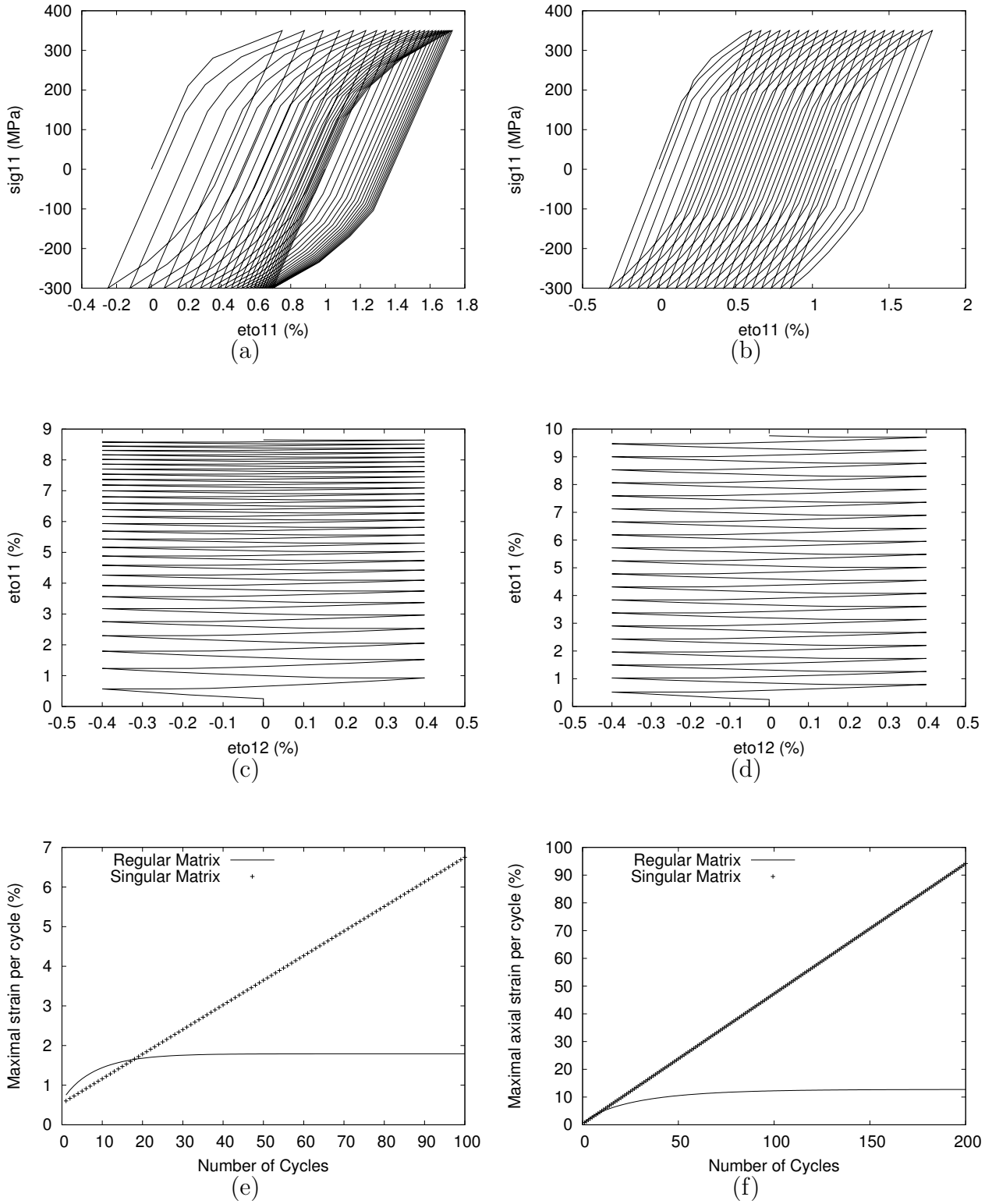

Fig. 2. Ratchetting behavior with linear kinematic hardening rules: (a) 1D loading under prescribed stress (-300 MPa, +350 MPa); ratchetting stopped by a regular matrix, (b) loading as in (a); ratchetting allowed by a singular matrix, (c) 2D loading, axial stress σ_{11}=250 MPa, prescribed shear strain $\varepsilon_{12} = \pm 0.4\%$; ratchetting stop allowed by a regular matrix, (d) loading as in (c) : ratchetting allowed by a singular matrix, (e) 1D Ratchetting: (f) 2D Ratchetting.

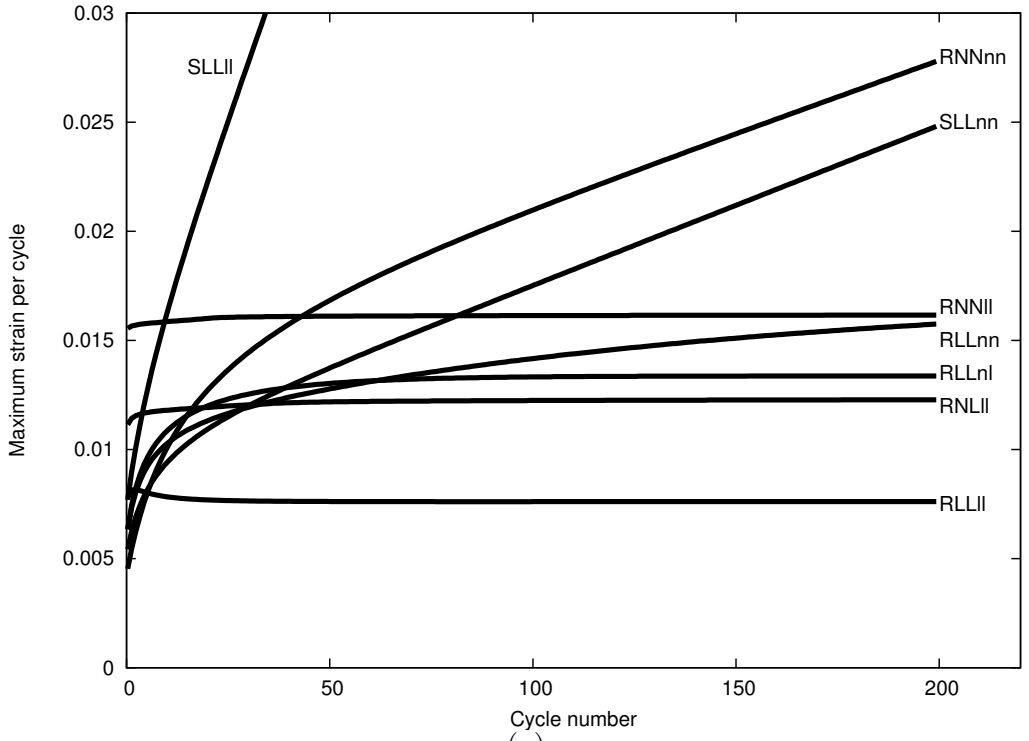

(a)

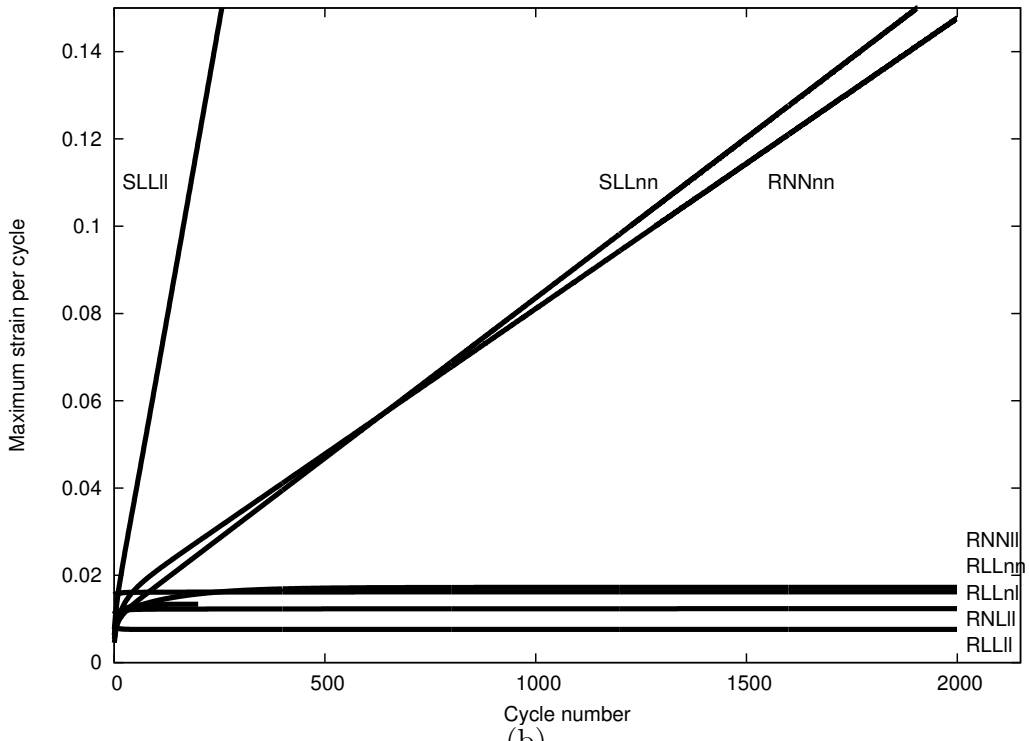

(b)

Fig. 3. Simulation of 1D ratchetting test using the 2M1C_β model under onedimensional loading prescribed axial stress (-150 MPa, +300 MPa): Systematic study of the effect of (i) the hardening matrix and (ii) the evolution rules of the kinematic hardening variables and the accomodation variables. (a) 200 cycles (b) 2000 cycles.

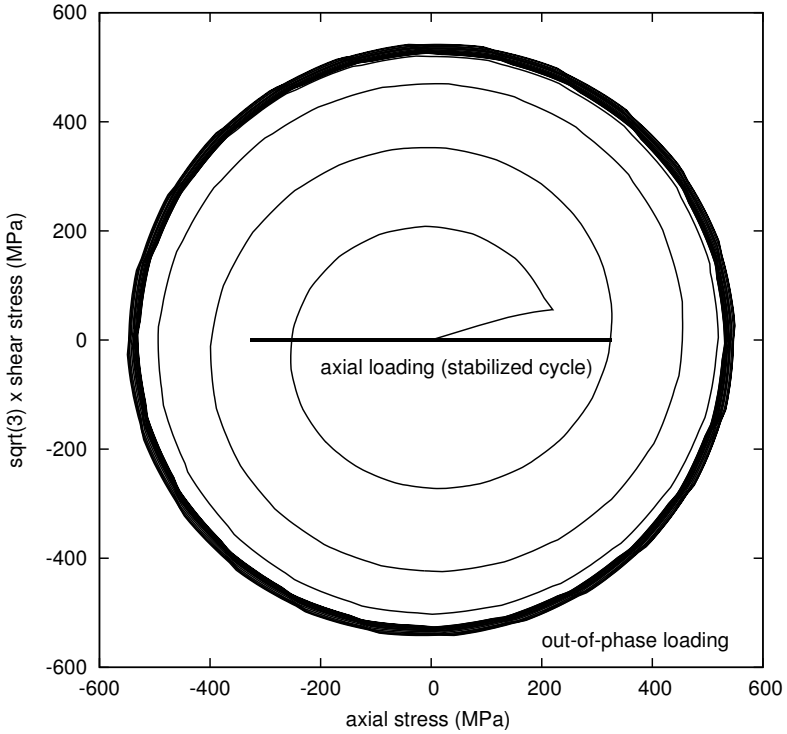

Fig. 4. Simulation of an out-of-phase test using the 2M1C_β–Model. The material parameters are almost the same used for the simulation of the 316 stainless steel behavior.

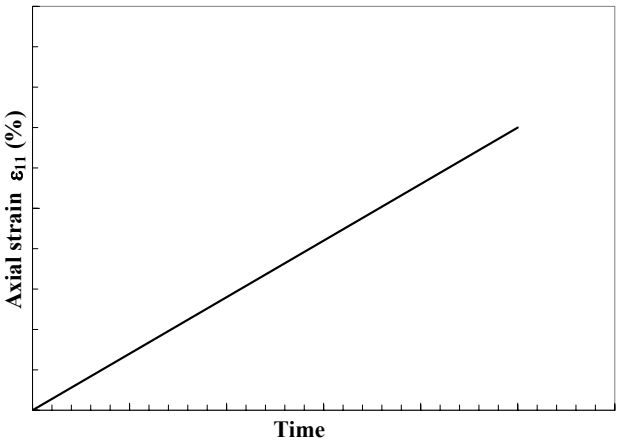

Monotonic tensile test

$\dot{\varepsilon} = 3.10^{-4} s^{-1}$.

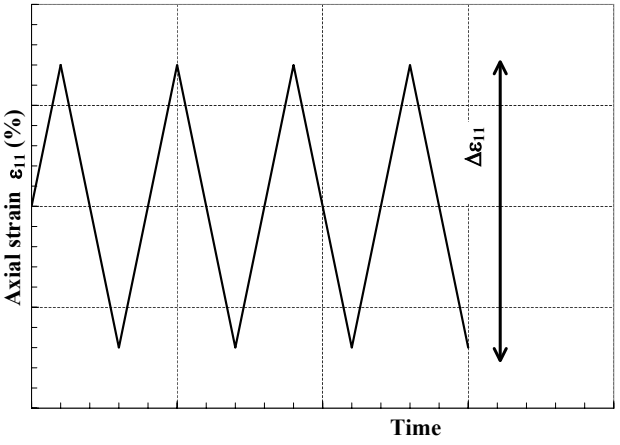

Cyclic loadings

$\Delta\varepsilon_{11} = 0.5, 0.65 \quad \text{and} \quad 0.8\%$

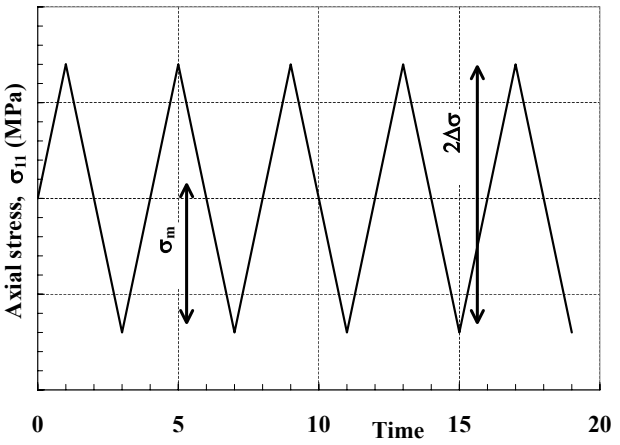

Tension ratchetting test

$\sigma_m = 100MPa, \Delta\sigma = 140MPa$

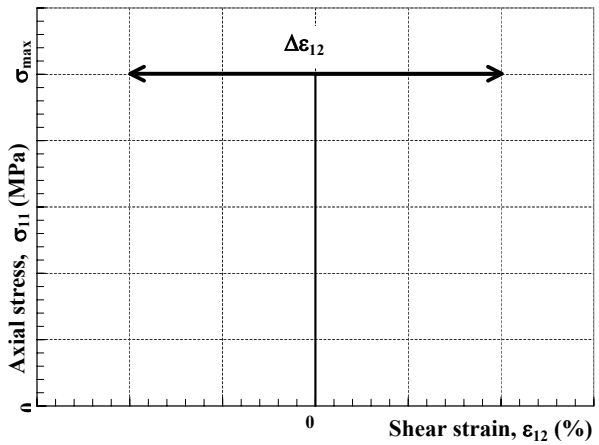

Tension-torsion ratchetting tests

$\sigma_{11} = 80MPa, \Delta\varepsilon_{12} = 0.1\%, 0.2\%, 0.5\%$

$\sigma_{11} = 100MPa, \Delta\varepsilon_{12} = 0.1\%, 0.2\%, 0.5\%$

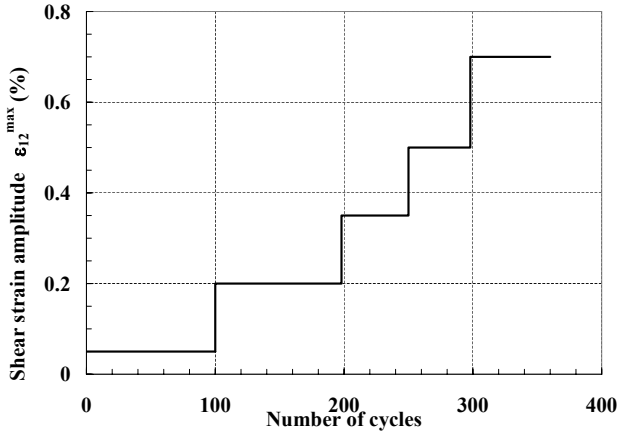

Tension-torsion ratchetting tests

$\sigma_{11} = 80MPa$, $\sigma_{11} = 100MPa$.

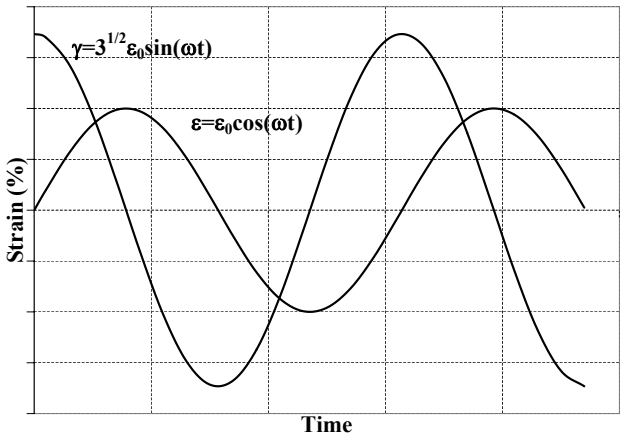

Tension-torsion out-of-phase test $\varepsilon_0 = 0.5\%$

Fig. 5. Description of the loading histories for the different tests of the experimental data base carried out by (Portier et al., 2000).

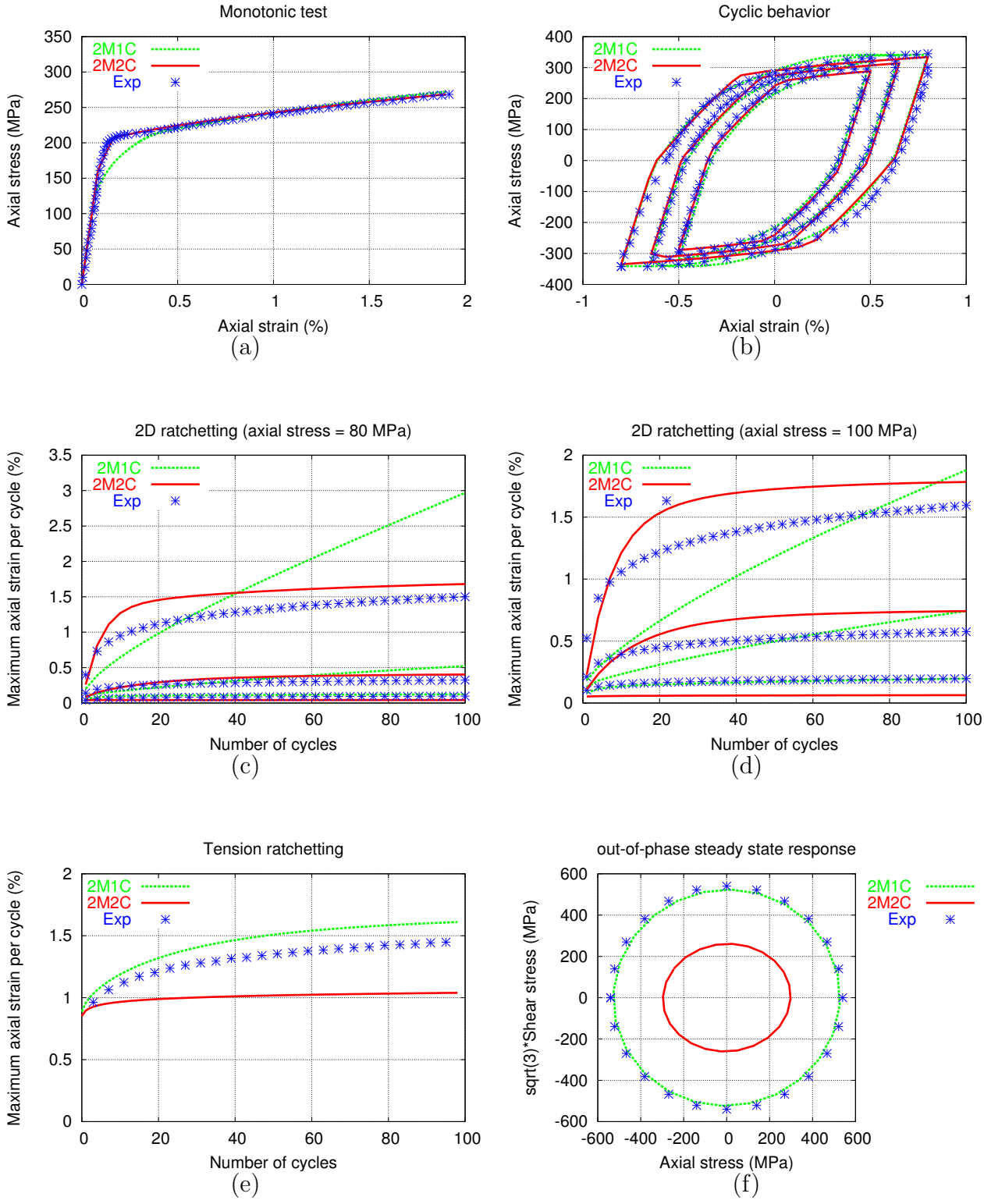

Fig. 6. Comparison between experiments test (Portier et al., 2000) and simulations for the 2M1C_β–Model: (a) Tensile test, (b) Cyclic behavior, (c) 2D Ratchetting, σ_{max} = 80 MPa with various $\Delta\epsilon_{12}$, (d) 2D Ratchetting, σ_{max} = 100 MPa with various $\Delta\epsilon_{12}$, (e) 1D Ratchetting, (f) Out of phase.

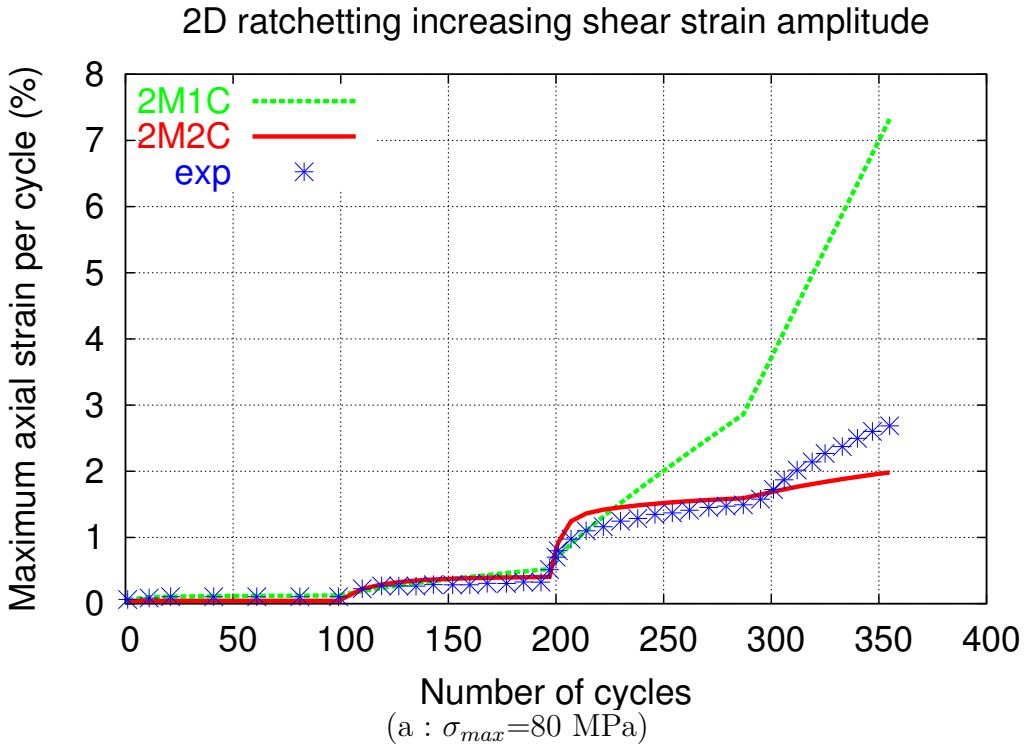

(a : σ_{max}=80 MPa)

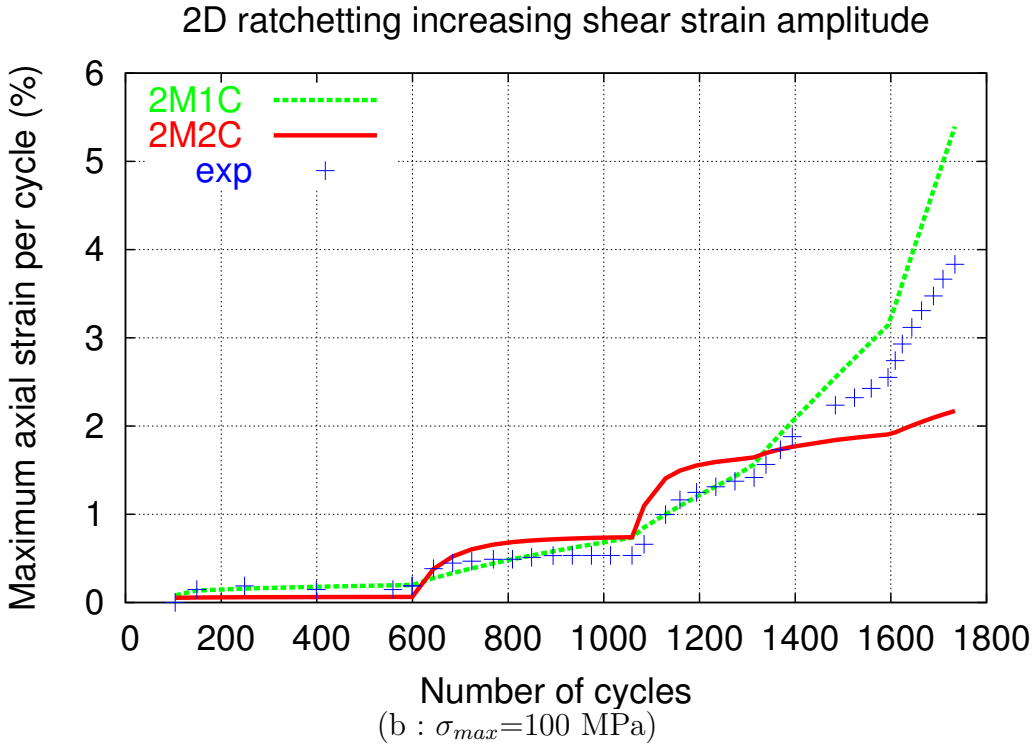

(b : σ_{max}=100 MPa)

Fig. 7. Validation of the 2M1C_β–Model: Tension-torsion ratchetting tests with increasing the shear strain amplitude.

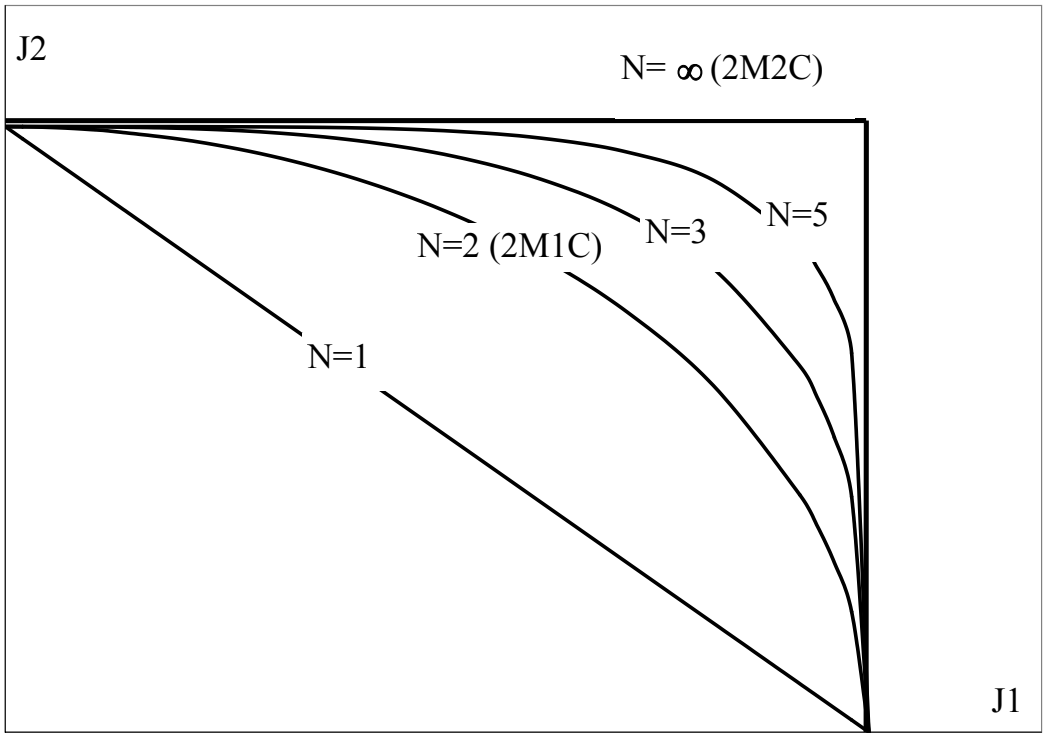

Fig. 8. Generalization of the 2M1C and the 2M2C models.

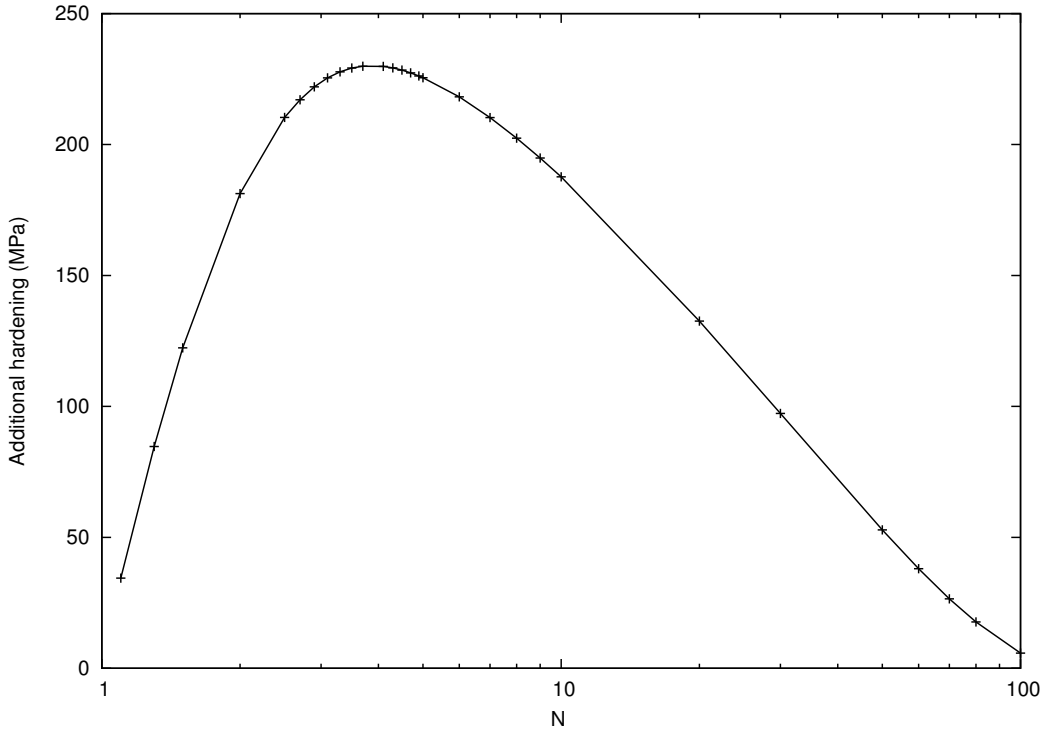

Fig. 9. Influence of the parameter N on the out-of-phase test.

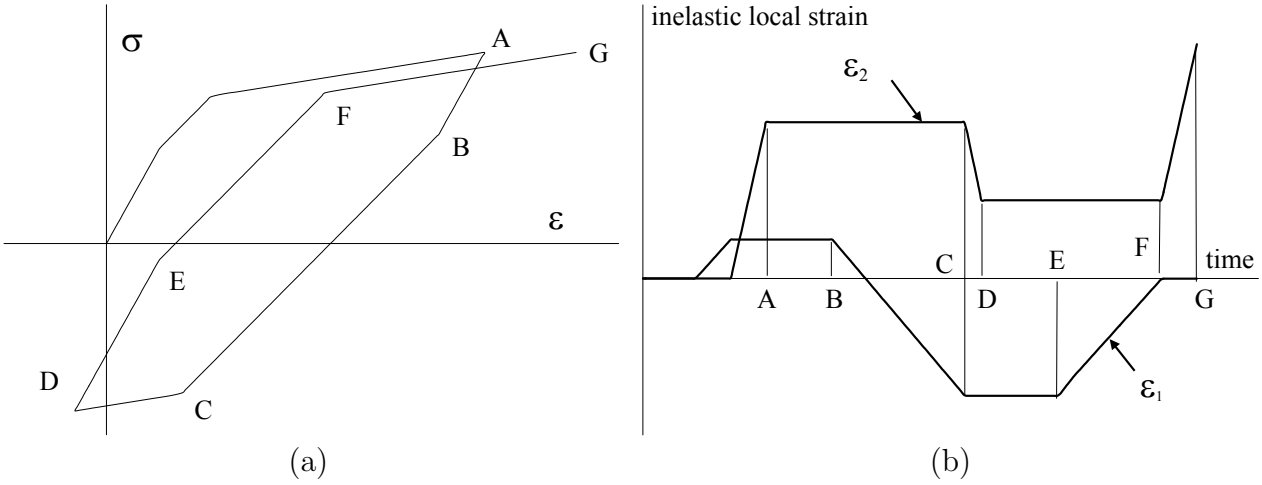

Fig. 10. Analytical study of the ratchetting behavior of the 2M2C model: (a) distinction of the different branches in the stress-strain loop, (b) activation of the mechanisms according to the different branches.

Appendix A

A Closed form solution for ratchetting behavior of the 2M2C model

- Case of linear kinematic hardening rule:

  Let us assume a one dimensional loading on a time-independent plasticity model with linear kinematic hardening rules and no isotropic hardening. We have the following equations:

$$\varepsilon^{in} = \varepsilon^1 + \varepsilon^2$$

$$f^1 = |\sigma - C_{11}\varepsilon^1 - C_{12}\varepsilon^2| - R_0^1$$

$$f^2 = |\sigma - C_{12}\varepsilon^1 - C_{22}\varepsilon^2| - R_0^2$$

$$\dot{\varepsilon}^1 = \dot{\lambda}^1 n^1$$

$$\dot{\varepsilon}^2 = \dot{\lambda}^2 n^2$$

$$n^1 = sign(\sigma - C_{11}\varepsilon^1 - C_{12}\varepsilon^2)$$

$$n^2 = sign(\sigma - C_{12}\varepsilon^1 - C_{22}\varepsilon^2)$$

  The purpose is to calculate the variation of the tensile peak strain between two successive cycles under applied cyclic stress (-σ_{min},+σ_{max}) (Fig. 10.a):

$$\delta\varepsilon^{in} = \varepsilon_G^{in} - \varepsilon_A^{in}$$

  If the stress σ_{max} is sufficiently high, the two mechanisms are simultaneously active. The conditions $f^I = 0$ lead to the system of two equations, in which

the unknowns are the local inelastic strains ε^1 and ε^2.

$$\begin{pmatrix} C_{11}\ C_{12} \\ \\ C_{12}\ C_{22} \end{pmatrix} \begin{pmatrix} \varepsilon^1 \\ \\ \varepsilon^2 \end{pmatrix} = \begin{pmatrix} \sigma_{max} - R_0^1 \\ \\ \sigma_{max} - R_0^2 \end{pmatrix} \tag{A.1}$$

If the determinant $C_{11}C_{22} - C_{12}^2 \neq 0$ then the local inelastic strains can be obtained from Eq. A.1:

$$\varepsilon_G^1 = \frac{(C_{22} - C_{12})\,\sigma_{max} + R_0^2 C_{12} - R_0^1 C_{22}}{C_{11}C_{22} - {C_{12}}^2} = \varepsilon_A^1 \tag{A.2}$$

$$\varepsilon_G^2 = \frac{(C_{11} - C_{12})\,\sigma_{max} + R_0^1 C_{12} - R_0^2 C_{11}}{C_{11}C_{22} - {C_{12}}^2} = \varepsilon_A^2 \tag{A.3}$$

Hence, a first property is obtained:

$$C_{11}C_{22} - C_{12}^2 \neq 0 \Rightarrow \delta\varepsilon^{in} = 0 \tag{A.4}$$

However, if $C_{11}C_{22} - C_{12}^2 = 0$ Eq. A.1 does not provide the inelastic strains. It can be noted:

· from A to B the behavior is purely elastic.

· from B to C only the first mechanism is active.

· from C to D the mechanism 2 is active and the coupling effect extinguishes the mechanism 1. As a matter of fact, the two consistency conditions $\dot{f}^1 = \dot{f}^2 = 0$ cannot be satisfied simultaneously. Using only the consistency condition $\dot{f}^2 = 0$ leads to $C_{12}\dot{\lambda}_1 + C_{22}\dot{\lambda}_2 = n^2\dot{\sigma}$. So that any positive value of $\dot{\lambda}^2$ gives a negative solution of $\dot{\lambda}^1$ because of the high value of C_{12} comparing to C_{22}. The only way to be consistent, is to assign $\dot{\lambda}^1$ to zero.

· from D to E the behavior is purely elastic.

· from E to F only mechanism 1 is active.

· from F to G the mechanism 2 is active and extinguishes the mechanism 1 for the same reasons explained before.

Fig. 10.b shows the evolution of the inelastic local strain of the two mechanisms corresponding to the stress-strain curve of the Fig. 10.a. In the one dimensional case, the yield surfaces are respectively taken as:

$$C_{11}\varepsilon^1 + C_{12}\varepsilon^2 = \sigma - n^1 R_0^1, \quad C_{12}\varepsilon^1 + C_{22}\varepsilon^2 = \sigma - n^2 R_0^2 \tag{A.5}$$

For the loading phase ($n^1 = n^2 = 1$), σ is equal to σ_{max}. Using $C_{11}C_{22} - C_{12}^2 = 0$ in Eq. A.5, the following expression is obtained:

$$C_{11}\varepsilon^1 + C_{12}\varepsilon^2 = \sigma_{max} - R_0^1 = \frac{C_{11}}{C_{12}}(\sigma_{max} - R_0^2) \tag{A.6}$$

The consistency conditions are respectively:

$$C_{11}\dot{\varepsilon}^1 + C_{12}\dot{\varepsilon}^2 = \dot{\sigma}, \quad C_{12}\dot{\varepsilon}^1 + C_{22}\dot{\varepsilon}^2 = \dot{\sigma} \tag{A.7}$$

Considering the above behaviors in different branches and using the property $C_{11}C_{22} - {C_{12}}^2 = 0$, the following results are obtained:

$$\varepsilon_F^1 = \varepsilon_B^1 + \frac{\sigma_F + \sigma_C - \sigma_E - \sigma_B}{C_{11}}, \quad \varepsilon_G^2 = \varepsilon_B^2 + \frac{\sigma_{max} + \sigma_{min} - \sigma_C - \sigma_F}{C_{22}} \tag{A.8}$$

with:

$$\sigma_F = \frac{C_{11}R_0^2 - C_{12}R_0^1}{C_{11} - C_{12}} \quad \text{and} \quad \sigma_C = \frac{C_{12}R_0^1 - C_{11}R_0^2}{C_{11} - C_{12}} \tag{A.9}$$

The stress state at B and E (end of branches with elastic behavior) is such that:

$$\sigma_B = -R_0^1 + \frac{C_{12}}{C_{22}}\left(\sigma_{max} - R_0^2\right) \tag{A.10}$$

$$\sigma_E = R_0^1 + \frac{C_{12}}{C_{22}}\left(\sigma_{min} + R_0^2\right) \tag{A.11}$$

Considering the expressions of these stresses, the variation of the tensile peak strain between two successive cycles can be deduced:

$$\delta\varepsilon^{in} = \left(\frac{1}{C_{22}} - \frac{1}{C_{12}}\right)(\sigma_{max} + \sigma_{min}) \quad \text{with} \quad C_{11}C_{22} - C_{12}^2 = 0 \tag{A.12}$$

The two following points should be emphasized:

· A shakedown behavior can also be obtained with a singular matrix in the special case $C_{11} = C_{12} = C_{22}$. In such a condition, the model degenerates into a single Chaboche's model and contains one back stress $\underset{\sim}{\mathbf{X}}$,

· The hardening modulus C_{22} must be less then C_{12} in the 2M2C model with a linear kinematic hardening rule and a singular matrix. Otherwise, a negative ratchetting may occurs with a high value of σ_{max}. By symmetry (using $C_{11}C_{22} - C_{12}^2 = 0$), C_{11} must be greater than C_{12}.

- Case of non linear kinematic hardening rule:

The variation of the tensile peak strain between two successive cycles cannot be obtained analytically for the kinematic hardening rule of Eq. 10. However, an analytic solution can be obtained if the dynamic recovery term $D_I \underset{\sim}{\alpha}_I$ is used instead of the term $(3/2)(D_I/C_{II})\underset{\sim}{\mathbf{X}}^I$:

$$\dot{\underset{\sim}{\alpha}}^I = \dot{\lambda}\left(\underset{\sim}{\mathbf{n}}^I - D_I \underset{\sim}{\alpha}^I\right) \quad (I = 1, 2) \tag{A.13}$$

The branches of the Fig. 10.a are now non linear and the following behaviors are considered:

· from A to B the behavior is purely elastic.

· from B to C only the first mechanism is active.

· from C to D the 2 mechanisms are active.

· from D to E the behavior is purely elastic.

· from E to F only the first mechanism is active.

· from F to G the 2 mechanisms are active.

The integration of the state variables between the different branches gives the following expression of the variation of the tensile peak strain:

$$\delta\varepsilon^{in} = \ln\left[\left(\frac{1 - D_1^2(\alpha_D^1)^2}{1 - D_1^2(\alpha_A^1)^2}\right)^{1/D_1}\left(\frac{1 - D_2^2(\alpha_D^2)^2}{1 - D_2^2(\alpha_A^2)^2}\right)^{1/D_2}\right] \tag{A.14}$$

In which α_A^1, α_D^1, α_A^2 and α_D^2 are the intermediate values of the kinematic hardening variables:

- $\alpha_A^1 = [(C_{22} - C_{12})\sigma_{max} + R_0^2 C_{12} - R_0^1 C_{22}]/(C_{22}C_{11} - C_{12}^2)$
- $\alpha_A^2 = [(C_{11} - C_{12})\sigma_{max} + R_0^1 C_{12} - R_0^2 C_{11}]/(C_{22}C_{11} - C_{12}^2)$
- $\alpha_D^1 = [(C_{22} - C_{12})\sigma_{min} - R_0^2 C_{12} + R_0^1 C_{22}]/(C_{22}C_{11} - C_{12}^2)$
- $\alpha_D^2 = [(C_{11} - C_{12})\sigma_{min} - R_0^1 C_{12} + R_0^2 C_{11}]/(C_{22}C_{11} - C_{12}^2)$

Eq. A.14 shows that the variation of the tensile peak strain is constant as in the unified model proposed by (Chaboche, 1986). This is not longer true if the kinematic hardening rule of Eq. 10 is considered.